

Powerful genome-wide design and robust statistical inference in two-sample summary-data Mendelian randomization

Qingyuan Zhao¹, Yang Chen, Jingshu Wang, Dylan S. Small

University of Pennsylvania, University of Michigan, University of Pennsylvania, University of Pennsylvania

Abstract: Background. Mendelian randomization (MR) uses genetic variants as instrumental variables to estimate the causal effect of risk exposures in epidemiology. Two-sample summary-data MR that uses publicly available genome-wide association studies (GWAS) summary data have become a popular design in practice. With the sample size of GWAS continuing to increase, it is now possible to utilize genetic instruments that are only weakly associated with the exposure.

Methods. To maximize the statistical power of MR, we propose a genome-wide design where more than a thousand genetic instruments are used. For the statistical analysis, we use an empirical partially Bayes approach where instruments are weighted according to their true strength, thus weak instruments bring less variation to the estimator. The final estimator is highly efficient in the presence of many weak genetic instruments and is robust to balanced and/or sparse pleiotropy.

Results. We apply our method to estimate the causal effect of body mass index (BMI) and major blood lipids on cardiovascular disease outcomes. Compared to previous MR studies, we obtain much more precise causal effect estimates and substantially shorter confidence intervals. Some new and statistically significant findings are: the estimated causal odds ratio of BMI on ischemic stroke is 1.19 (95% CI: 1.07–1.32, p -value ≤ 0.001); the estimated causal odds ratio of high-density lipoprotein cholesterol (HDL-C) on coronary artery disease (CAD) is 0.78 (95% CI 0.73–0.84, p -value ≤ 0.001). However, the estimated effect of HDL-C becomes substantially smaller and statistically non-significant when we only use the strong instruments.

Conclusions. By employing a genome-wide design and robust statistical methods, the statistical power of MR studies can be greatly improved. Our empirical results suggest that, even though the relationship between HDL-C and CAD appears to be highly heterogeneous, it may be too soon to completely dismiss the HDL hypothesis. Further investigations are needed to demystify the observational and genetic associations between HDL-C and CAD.

Keywords: Conditional score, HDL hypothesis, Partially Bayes, Robust statistics, Spike-and-slab prior.

Key messages:

- We utilize common variants across the whole genome (typically over a thousand) as instrumental

¹Address for correspondence: Department of Statistics, The Wharton School, University of Pennsylvania, Jon M. Huntsman Hall, 3730 Walnut Street, Philadelphia, PA 19104-6340 USA. E-mail: qyzhao@wharton.upenn.edu. Nov. 16, 2018.

variables.

- We extend a previously proposed method—robust adjusted profile score—to account for the measurement error in GWAS summary data and biases due to weak instruments. A new method—empirical partially Bayes—is developed to increase the statistical power when some genetic instruments are strong but many are very weak. The estimator is robust to balanced and/or sparse pleiotropy.
- Our new and more powerful analysis greatly improves the precision of the causal effect estimates of BMI and blood lipids on cardiovascular disease outcomes.
- Code to replicate the results (including diagnostics) is available in the R package `mr.raps` (<https://github.com/qingyuanzhao/mr.raps>).

1 Introduction

Mendelian randomization (MR) is a method of using genetic variation to infer the causal effect of a modifiable risk exposure on disease outcome. Since MR can give unbiased estimates in the presence of unmeasured confounding, it has become a widely used tool for epidemiologists and health scientists [1]. A prominent example is the overwhelming evidence of a causal link between low-density lipoprotein cholesterol (LDL-C) and coronary heart disease found by several MR studies [2, 3, 4, 5], which is consistent with the results of earlier landmark clinical trials [6].

From a statistical perspective, MR is a special instance of instrumental variable (IV) methods [7, 8]. Compared to classical applications of the IV methods in economics [9] and health research [10], the most distinctive feature of MR is the enormous number of candidate instruments. Potentially, any one of the millions of single nucleotide polymorphisms (SNP) in the human genome can be used as an IV as long as it satisfies the following three validity criteria [10]:

1. Relevance: the SNP must be associated with the risk exposure.
2. Effective random assignment: the SNP must be independent of any unmeasured confounder that is a common cause of the exposure and outcome under investigation.
3. Exclusion restriction (ER): the SNP affects outcome only through the risk exposure.

Among the three criteria above, the ER assumption is most disputable for MR due to a widespread phenomenon called pleiotropy [11, 12], a.k.a. multiple functions of genes. For example, there are many SNPs that are associated with both LDL-C and high-density lipoproteins cholesterol (HDL-C), thus their effects on cardiovascular outcomes are possibly mediated by both lipids. When these SNPs are used as instruments in a MR analysis of HDL-C, the ER assumption is likely violated.

To alleviate these concerns, most existing MR studies [13, 14, 15] select a handful of genome-wide significant SNPs that are associated with the exposure risk factor and then seek to justify that the ER assumption is reasonable. This simple design is very transparent, but it has some major limitations. First, a full justification of the ER assumption requires a deep understanding of the causal mechanism of the genes and can be invalidated by new findings. For example, Katan [16], an early exponent of MR, proposed to use polymorphic forms of the *APOE* gene to estimate the causal effect of blood cholesterol on cancer. However, as Davey Smith and Ebrahim [17] later argued, they may be invalid instruments due to pleiotropic effects on other biomarkers. Second,

the statistical power of MR is substantially reduced when the vast majority of SNPs are excluded, including a lot of known genetic variation of the exposure and the outcome (Figure 1).

Meanwhile, it is well known to econometricians and statisticians that weak IVs can still provide valuable information, especially if there are a number of them [18, 19]. In a previous paper [20], we found that using weakly significant SNPs can greatly increase the efficiency of MR studies. In a different but related application, Bulik-Sullivan et al. [21] also found that a genome-wide analysis is much more powerful than using just the significant SNPs to estimate the genetic correlation. Using weak instruments also helps to test the presence of effect heterogeneity [22] and identify candidate IVs that do not satisfy the ER assumption, and the causal effect can still be consistently estimated when the invalid IVs are rare or the pleiotropic effects are balanced [20, 23, 24, 25].

In this paper, we will introduce two new strategies that can greatly increase the statistical power of MR studies. The first innovation is a truly genome-wide design: unlike previous MR studies including our earlier work [20], no threshold will be used in the selection phase (apart from demanding the genetic instruments to be independent). Typically, about 1000 independent genetic instruments will be used in a genome-wide MR study. Notice that a genetic variant is considered to satisfy the first IV assumption (relevance) even if it does not causally modify the exposure. The variant can be used as an IV if it is in linkage disequilibrium with a causal variant and thus associated with the exposure [7]. The blueprint of genome-wide MR has been discussed in the literature before [26, 27, 28], but it was not feasible until recently because most existing summary-data MR methods are heavily biased by weak IVs.

Our second innovation is an estimator that adaptively assigns weights to the IVs according to their strength. This method is based on a general empirical partially Bayes approach introduced by Lindsay [29]. Our previous method of adjusting the profile score [20] can be viewed as a special case of this approach using a predetermined flat prior. Both approaches yield consistent and asymptotically normal estimators of the causal effect, but using an empirically estimated prior can substantially increase the statistical power. The structure of the empirical partially Bayes approach also motivates a new diagnostic plot and a hypothesis test that is useful to detect effect heterogeneity according to instrument strength.

2 Genome-wide design

We will use a working example to illustrate the genome-wide MR design, where the goal is to estimate the causal effect of body mass index (BMI) on the risk of CAD. Increased adiposity was

found to increase the risk of CAD in several previous MR studies [30, 31, 32, 33]. In this paper we use this example as a positive control to demonstrate how using weak instruments can greatly improve the precision of MR.

Our two-sample summary-data MR design makes use of three non-overlapping GWAS:

1. **Selection dataset:** A GWAS for BMI in the Japanese population involving 173,430 individuals [34];
2. **Exposure dataset:** A GWAS for BMI in the UK BioBank involving more than 350,000 individuals [35];
3. **Outcome dataset:** A GWAS for CAD conducted by the CARDIoGRAMplusC4D consortium of about 185,000 cases and controls with genotype imputation using the 1000 Genomes Project [36].

For each GWAS, the summary data are publicly available, which report the linear or logistic regression coefficients and standard errors (typically following a meta-analysis) of all the genotyped or imputed SNPs. The **selection** and **exposure** datasets are two non-overlapping GWAS for the same (or similar) phenotypes. We recommend to reserve the GWAS with higher quality (e.g. larger sample size, same population as the **outcome dataset**) for the **exposure** dataset. The quality of the **selection dataset** is often less important with a genome-wide MR design.

After obtaining the GWAS summary datasets, we preprocess the data to select genetic instruments for the statistical analysis. We first remove SNPs that do not coappear in all three datasets. Then we use the remaining **selection dataset** to find independent SNPs (distance ≥ 10 megabase pairs, linkage disequilibrium $R^2 \leq 0.001$) that are most associated with BMI. This is done in a greedy fashion using the linkage-disequilibrium (LD) clumping function in the PLINK software [37]. Using independent SNPs makes the statistical analysis more convenient and is common in MR studies [15]. Suppose p SNPs are selected after LD clumping. Usually p is about 1000 after the described preprocessing; in our working example concerning BMI and CAD, $p = 1119$.

A typical summary-data MR dataset thus consists of $2p$ marginal genetic effect estimates (linear/logistic regression coefficients) and their standard errors from the exposure and outcome datasets:

- $\hat{\gamma}_j, j = 1, \dots, p$ are the genetic effects on the exposure (BMI). The standard errors are denoted by σ_{Xj} .

- $\hat{\Gamma}_j, j = 1, \dots, p$ are the genetic effects on the outcome (CAD). The standard errors are denoted by σ_{Yj} .

The study design described above is usually called a two-sample summary-data MR study [38]. Here we want to emphasize that using a separate and non-overlapping dataset for SNP selection is very important for the unbiasedness of the genetic effect estimates, thus eliminating any bias due to “winner’s curse” [39]. A common misconception is that, when the same GWAS is used for selection and to obtain $\hat{\gamma}_j$, the “winner’s curse” could be avoided by only using genome-wide significant SNPs. This is not true, because although these SNPs are most likely true hits, the estimated genetic effects $\hat{\gamma}_j$ are still biased. As a consequence, the causal effect estimate is generally biased towards zero [20].

Figure 1 shows the distribution of genetic signal strength measured by the squared l_2 norm $\|\boldsymbol{\gamma}\|^2 = \sum_{j=1}^p \gamma_j^2$ (for BMI) and $\|\boldsymbol{\Gamma}\|^2$ (for CAD) as a function of the selection threshold. Throughout the paper we use bold letters to indicate vectors. These quantities are closely related to the genetically inherited phenotypic variance and can be unbiasedly estimated by $\sum_j \hat{\gamma}_j^2 - \sigma_{Xj}^2$ and $\sum_j \hat{\Gamma}_j^2 - \sigma_{Yj}^2$ over the SNPs that pass the selection threshold. Compared to the conventional analysis that only uses 44 genome-wide significant SNPs (p -value $\leq 5 \times 10^{-8}$), the genome-wide MR design using all the 1119 SNPs contains almost twice amount of genetic variation for BMI. This observation suggests a great potential of increasing the statistical power of the MR analysis by utilizing the weaker instruments.

3 Statistical model

Following our previous article [20], our main modeling assumptions are:

Assumption 1 (Measurement error model).

$$\begin{pmatrix} \hat{\gamma} \\ \hat{\Gamma} \end{pmatrix} \sim N \left(\begin{pmatrix} \gamma \\ \Gamma \end{pmatrix}, \begin{pmatrix} \boldsymbol{\Sigma}_X & \mathbf{0} \\ \mathbf{0} & \boldsymbol{\Sigma}_Y \end{pmatrix} \right), \quad \boldsymbol{\Sigma}_X = \text{diag}(\sigma_{X1}^2, \dots, \sigma_{Xp}^2), \quad \boldsymbol{\Sigma}_Y = \text{diag}(\sigma_{Y1}^2, \dots, \sigma_{Yp}^2).$$

Assumption 2 (Pleiotropy model). *We assume the causal effect β satisfies $\Gamma_j \approx \beta\gamma_j$ for most $j = 1, \dots, p$. More specifically, let $\boldsymbol{\alpha} = \boldsymbol{\Gamma} - \beta\boldsymbol{\gamma}$. We assume α_j is independent of γ_j and most $\alpha_j \stackrel{\text{ind}}{\sim} N(0, \tau^2)$ where τ^2 is a small overdispersion parameter. A small proportion of the SNPs (say 5%) might deviate from this model and have very large $|\alpha_j|$.*

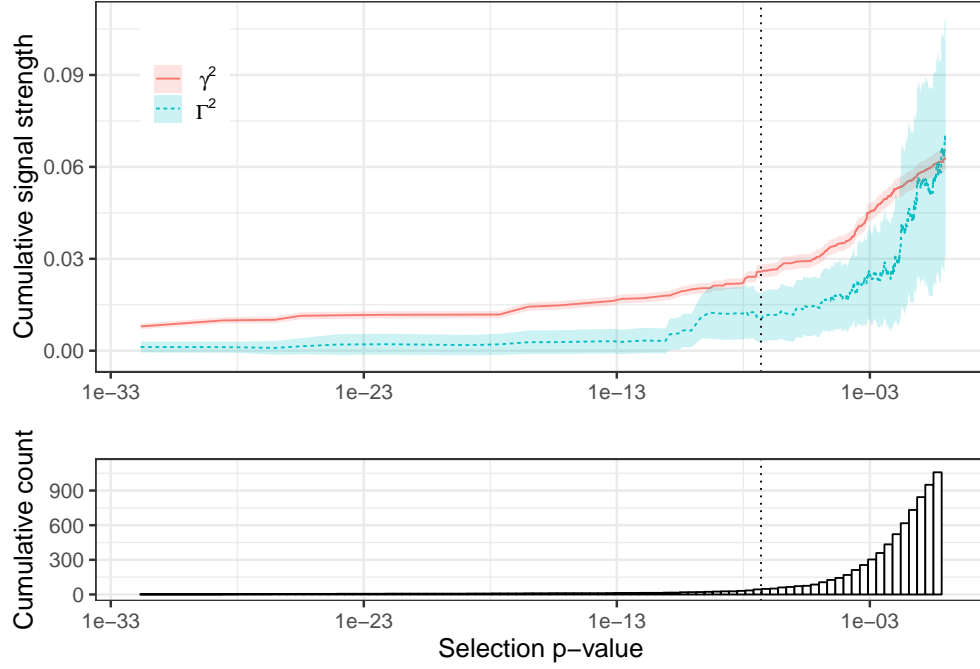


Figure 1: Distribution of signal strength in the genome-wide MR of Body Mass Index (BMI) on Coronary Artery Disease (CAD) as a function of the selection p -value: $\sum_{\text{SNP } j \text{ pass threshold}} \gamma_j^2$ and $\sum_{\text{SNP } j \text{ pass threshold}} \Gamma_j^2$. See Section 5 below for more details of this dataset. Shaded region in the main plot is 95% confidence interval of the estimated cumulative signal strength. The dotted vertical line corresponds to the standard genome-wide significance threshold 5×10^{-8} in the selection dataset.

The normality and independence assumptions in Assumption 1 can be immediately justified by the large sample size of GWAS, non-overlapping samples in the **selection**, **exposure**, and **outcome datasets**, and independence of the SNPs [20]. We have also implicitly assumed that the standard errors σ_{Xj} , σ_{Yj} , $j = 1, \dots, p$ reported in the GWAS are well calibrated.

Assumption 2 presumes that for most SNPs, the genetic associations with the exposure and the outcome approximately satisfy a pair-wise linear relationship, with the common slope parameter being the causal effect β . When all the SNPs are valid IVs, the linear relationship $\mathbf{\Gamma} = \beta\boldsymbol{\gamma}$ can be derived through assuming the SNPs, exposure and outcome variables follow a linear structural model [40]. This result can be extended to nonlinear structural models by assuming the per-SNP effects are minuscule and the SNPs affect the exposure in a homogenous way [20]. When the outcome variable is the binary disease status, β may be interpreted as a conservative estimate of the causal log-odds-ratio [20].

In reality, many genetic variants may violate the ER assumption and have other pathways to affect CAD. For example, a SNP selected for the MR study of HDL-C might also be associated with LDL-C, so its genetic association with CAD includes both the causal effect of HDL-C (if any) and LDL-C. Motivated by the exploratory analysis for the MR of adiposity on blood pressure in our previous paper [20], the robust MR model in Assumption 2 considers two types of deviations from the exact linear relationship $\mathbf{\Gamma} = \beta\boldsymbol{\gamma}$: 1. small and balanced pleiotropy represented by the random effects model $\alpha_j \sim N(0, \tau^2)$; 2. idiosyncratic and large pleiotropy. The first kind of deviation is a special case of the InSIDE (Instrument Strength Independent of Direct Effect) assumption [40, 41], while the second is similar to the sparse invalid IV assumption [23]. We think it is crucial that the statistical method of MR is robust to both kinds of pleiotropy.

As a remark, when the InSIDE assumption is not satisfied, the causal effect β cannot be identified without further assumptions. In this case, the estimand of our statistical method below is β plus $(\boldsymbol{\gamma}^T \boldsymbol{\gamma})^{-1} \boldsymbol{\gamma}^T \boldsymbol{\alpha}$, the regression slope of $\boldsymbol{\alpha}$ on $\boldsymbol{\gamma}$.

Before diving into the details of our statistical methodology, we want to mention that an alternative approach to handle widespread pleiotropy is the multivariable MR [42, 43], where several exposures are examined simultaneously. In the rest of this paper we will focus on the genome-wide design for univariate MR and explore the multivariate extension in a forthcoming work.

4 Statistical method

In our previous article [20], we proposed a robust estimator based on adjusting the profile score function of β and τ^2 , in which the nuisance parameters γ are profiled out. Here we propose a new method to eliminate the nuisance parameters γ based on an empirical partially Bayes approach introduced by Lindsay [29]. The new method has a simple geometric interpretation and can further increase the statistical power.

4.1 Empirical partially Bayes

We first consider the simplest scenario: $\alpha = \mathbf{0}$. The key insight is gained from deriving the contribution of the j -th SNP to the conditional score function (Appendix A):

$$C_j(\beta, \gamma_j) = \frac{\gamma_j(\hat{\Gamma}_j - \beta\hat{\gamma}_j)}{\beta^2\sigma_{Xj}^2 + \sigma_{Yj}^2}.$$

It is straightforward to verify that the maximum likelihood estimator (MLE) of γ_j given β , denoted as $\hat{\gamma}_{j,\text{MLE}}(\beta)$, is a sufficient statistic of γ_j and is independent of $\hat{\Gamma}_j - \beta\hat{\gamma}_j$. The decoupling of “instrument strength” γ_j and “regression residual” $\hat{\Gamma}_j - \beta\hat{\gamma}_j$ in $C_j(\beta, \gamma_j)$ motivates us to consider a general class of estimating functions:

$$C(\beta) = \sum_{j=1}^p \frac{f_j(\beta, \hat{\gamma}_{j,\text{MLE}}(\beta)) \cdot \psi(t_j(\beta))}{\sqrt{\beta^2\sigma_{Xj}^2 + \sigma_{Yj}^2}}, \quad t_j(\beta) = \frac{\hat{\Gamma}_j - \beta\hat{\gamma}_j}{\sqrt{\beta^2\sigma_{Xj}^2 + \sigma_{Yj}^2}},$$

where f_j is an arbitrary function of β and $\hat{\gamma}_{j,\text{MLE}}$, and ψ is an odd function (so $\psi(-t) = -\psi(t)$). Because $\hat{\gamma}_{j,\text{MLE}}(\beta)$ is independent of $\hat{\Gamma}_j - \beta\hat{\gamma}_j$ (and thus $t_j(\beta)$), it is easy to show that $\mathbb{E}[C(\beta)] = 0$ at the true β . Therefore the root of $C(\beta)$, denoted by $\hat{\beta}$, is a reasonable estimator of β . Geometrically, this estimating function finds the β such that a transformation (by f) of the estimated “instrument strength” $\hat{\gamma}_{j,\text{MLE}}(\beta)$ is uncorrelated with a transformation (by ψ) of the “regression residual” $\hat{\Gamma}_j - \beta\hat{\gamma}_j$.

Different choices of the weighting scheme f_j do not change the unbiasedness of $C(\beta)$, but may affect the statistical efficiency. The profile score developed in our previous article [20] amounts to using $\hat{\gamma}_{j,\text{MLE}}(\beta)$ as the weight. To maximize statistical power, Lindsay [29] suggested to use the empirical Bayes estimate of γ_j as the weight,

$$f_j(\beta, \hat{\gamma}_{j,\text{MLE}}(\beta)) = \hat{\gamma}_{j,\text{EB}}(\beta) = \mathbb{E}_{\pi_{\hat{\gamma}}}[\gamma_j | \hat{\gamma}_{j,\text{MLE}}(\beta)]$$

where π_η is a prior distribution of γ and $\hat{\eta}$ is an empirical estimate of the prior parameter. Intuitively, $\hat{\gamma}_{j,\text{EB}}$ shrinks $\hat{\gamma}_{j,\text{MLE}}$ towards 0. The function ψ is chosen to limit the influence of large outliers (Section 4.3).

4.2 Spike-and-slab prior

In principle, a good choice of the prior distribution π_η should have the following properties: 1. the parametric family π_η should fit the distribution of γ reasonably well, so we can gain efficiency by using the empirical partially Bayes estimator; 2. The empirical Bayes estimator of γ_j should be easy to compute since it will be evaluated many times when iteratively solving the estimating equations. For these reasons, we choose to use a spike-and-slab Gaussian mixture prior [44, 45] to model γ_j/σ_{Xj} in all our empirical examples:

$$\gamma_j/\sigma_{Xj} \sim \pi_{p_1, \sigma_1, \sigma_2} = p_1 \cdot \text{N}(0, \sigma_1^2) + (1 - p_1) \cdot \text{N}(0, \sigma_2^2).$$

We decide to model the effect sizes γ_j/σ_{Xj} instead of the effects γ_j because this scale is more familiar and the shrinkage rule is easier to interpret. Typically, p_1 is close to 1, σ_1^2 is close to zero (the spike component), and σ_2^2 is much larger than σ_1^2 (the slab component). The selective shrinkage offered by the spike-and-slab prior [46] is essential to gain efficiency in empirical partially Bayes (Appendix A.2).

4.3 Robust estimator

To account for invalid IVs in Assumption 2, we need to further estimate the overdispersion parameter $\tau^2 = \text{Var}(\alpha_j)$ while being robust to large outliers of α_j . Intuitively, we need two estimating equations after eliminating the nuisance γ : one for β and one for τ^2 . For β , we can follow the empirical partially Bayes approach described above by replacing σ_{Yj}^2 with $\sigma_{Yj}^2 + \tau^2$. For τ^2 , we need to adjust the profile score function of τ^2 due to a Neyman-Scott phenomenon [20, 47]. To be robust against outliers, we propose to use a bounded function of the “regression residual” $\hat{\Gamma}_j - \beta \hat{\gamma}_j$.

Next we describe the robust estimating function of β and τ^2 . Derivation of these functions is very similar to our previous RAPS (Robust Adjusted Profile Score) approach [20] and the details are omitted. Let $\psi_1(\cdot)$ and $\psi_2(\cdot)$ be two differentiable odd functions. The empirical partially Bayes version of the RAPS estimator $(\hat{\beta}, \hat{\tau}^2)$ is given by the solution to $\tilde{\mathbf{C}}(\beta, \tau^2) = (\tilde{C}_1(\beta, \tau^2), \tilde{C}_2(\beta, \tau^2))^T =$

$\mathbf{0}$, where

$$\begin{aligned}\tilde{C}_1(\beta, \tau^2) &= \sum_{j=1}^p \frac{\hat{\gamma}_{j,\text{EB}}(\beta, \tau^2) \cdot \psi_1(t_j(\beta, \tau^2))}{s_j(\beta, \tau^2)}, \text{ and} \\ \tilde{C}_2(\beta, \tau^2) &= \sum_{j=1}^p \frac{\psi_2(t_j(\beta, \tau^2)) - \delta}{s_j^2(\beta, \tau^2)}, \text{ where } \delta = \mathbb{E}[\psi_2(Z)] \text{ for } Z \sim \text{N}(0, 1),\end{aligned}$$

where $t_j(\beta, \tau^2) = (\hat{\Gamma}_j - \beta \hat{\gamma}_j)/s_j(\beta, \tau^2)$ is the standardized regression residual and $s_j(\beta, \tau^2) = \sqrt{\beta^2 \sigma_{X_j}^2 + \sigma_{Y_j}^2 + \tau^2}$.

In the empirical examples below, we will use $\psi_2(t) = t \cdot \psi_1(t)$ and consider two choices of ψ_1 : the non-robust identity function ψ_I and the robust Huber's score function ψ_H . A situation we sometimes encounter with real data is that the RAPS estimating equation may have several roots. In this case, we report the root closest to the optimization-based profile-likelihood estimator if there no other close root; otherwise we simply report the empirical partially Bayes estimator is not available. We do not interpret this as a defect of the proposed method; rather, there is often strong evidence for effect heterogeneity in this situation and we think the investigator should avoid making any hasty conclusion. Further implementation details including how to compute the standard error of $\hat{\beta}$ can be found in Appendix A.2.

4.4 Diagnostics

A potential concern of using many weak instruments is that they might have more pleiotropy than strong instruments [12, 48]. It is possible that the covariance $\text{Cov}(\alpha_j, \gamma_j)$ is a function of the instrument strength γ_j and is non-zero for certain range of γ_j (under Assumption 2 or more generally the InSIDE assumption, $\text{Cov}(\alpha_j, \gamma_j) \approx 0$). In general, the conclusions of a genome-wide MR study are stronger if the weak instruments and strong instruments produce similar estimates of the causal effect. We propose a simple diagnostic plot for this purpose, where the standardized regression residual $t_j(\beta, \tau^2)$ is plotted against (a standardized version of) the estimated instrument strength

$$\hat{\gamma}_{j,\text{EB}}(\beta, \tau^2) / \sqrt{\text{Var}(\hat{\gamma}_{j,\text{EB}}(\beta, \tau^2))},$$

evaluated at $(\beta, \tau^2) = (\hat{\beta}, \hat{\tau}^2)$. At the true value of (β, τ^2) and when our modeling assumptions are satisfied, t_j should be independent of $\hat{\gamma}_{j,\text{EB}}$ and follow a standard normal distribution (possibly with some outliers). This proposition can be empirically checked in a diagnostic plot (Appendices A.2.5

and C.2). Furthermore, it can be used to test for the heterogeneity of the instruments. In our empirical studies, we report the heterogeneity p -value as the null test for the linear regression of standardized residuals on estimated instrument strength (expanded using B-splines with degrees of freedom equal to $p/20$). This can be used as a falsification test of our modeling assumptions. A related but different graphical outlier detection method is the radial MR plot proposed by Bowden et al. (2018) [49].

5 Datasets

Table 1a summarizes the datasets used in our empirical studies. We will consider 6 phenotypes: BMI, LDL-C, HDL-C, triglycerides (TG), CAD (or myocardial infarction), and ischemic stroke (IS), and apart from IS, all other phenotypes have at least two non-overlapping GWAS results. Table 1b lists the design of the empirical examples in the next two sections.

In our genome-wide MR design, we require the **selection**, **exposure**, and **outcome** GWAS to have non-overlapping samples. Often the GWAS summary results are based on meta analyses of smaller cohorts, so this assumption can be examined by checking if they have no common participating cohort. This is the case for most of our empirical examples below. The only exception is the MR analysis of the blood lipids and CAD, where the **outcome dataset** obtained from the CARDIoGRAMplusC4D consortium overlaps with the lipids GWAS reported by the GLGC consortium. Nevertheless, the sample overlap appears to be small by examining the participating cohorts.

The amount of sample overlap can also be tested by running the LD score regression [55]. Bulik-Sullivan et al. (2015) [21] show that the intercept in the LD score regression is proportional to the amount of sample overlap, and the slope in the regression is proportional to the genetic correlation. Figure 2 shows the results of the LD score regression for the datasets used in this paper. The regression intercepts between the lipids datasets and CAD are relatively small and not statistically significant, indicating the amount of sample overlap may be small.

6 Validation studies

6.1 Simulations

We perform two validation studies of the proposed statistical method. The first is a simulation study that mimics the real data analysis for LDL-C and CAD using restricted instruments (Table C3a). The GWAS summary data are simulated according to Assumptions 1 and 2 in six settings: NOO

Phenotype	Dataset name	Citation or data source	Population	Sample size
BMI	BMI (Jap)	Akiyama et al. (2017) [34]	Asian	173,430
	BMI (UKB)	UK BioBank [35]	European	> 350,000
Lipids	LDL (2010)	Teslovich et al. (2010) [50]	European	$\sim 100,000$
	HDL (2010)			
	TG (2010)			
	LDL (2013)	Global Lipids Genetics Consortium (2013) [51]	European	$\sim 100,000$
	HDL (2013)			
	TG (2013)			
CAD	CARDIoGRAM	Schunkert et al. (2011) [52]	European	86,995
	C4D	C4D Genetics Consortium (2011) [53]	European and South Asian	30,442
	CAD	CARDIoGRAMplusC4D Consortium (2015) [36]	European	$\sim 185,000$
Myocardial Infarction	MI (UKB)	UK BioBank [35]	European	> 350,000
Ischemic Stroke	IS	Malik et al. (2018) [54]	European	446,696

(a) List of publicly available GWAS summary datasets used in this paper. See Appendix B for web links we used to download the datasets.

Study name	Screening dataset	Exposure dataset	Outcome dataset	Results
Simulations	Data are simulated to mimic the MR analysis for the LDL-CAD study below.			Section 6.1; Table 2
CAD-CAD	MI (UKB)	C4D	CARDIoGRAM	Section 6.2; Table 3
BMI-CAD BMI-IS	BMI (Jap)	BMI (UKB)	CAD IS	Section 7.1; Tables 4 and C1; Figures 3 and C1
LDL-CAD HDL-CAD TG-CAD	LDL (2010) HDL (2010) TG (2010)	LDL (2013) HDL (2013) TG (2013)	CAD	Section 7.2; Tables 5, C2 and C4; Figures 3, C2 and C3
LDL-MI HDL-MI TG-MI	LDL (2010) HDL (2010) TG (2010)	LDL (2013) HDL (2013) TG (2013)	MI (UKB)	Section 7.2; Tables 5, C3 and C5; Figures C4 and C5

(b) List of MR analyses.

Table 1: GWAS Datasets and MR analyses in this paper.

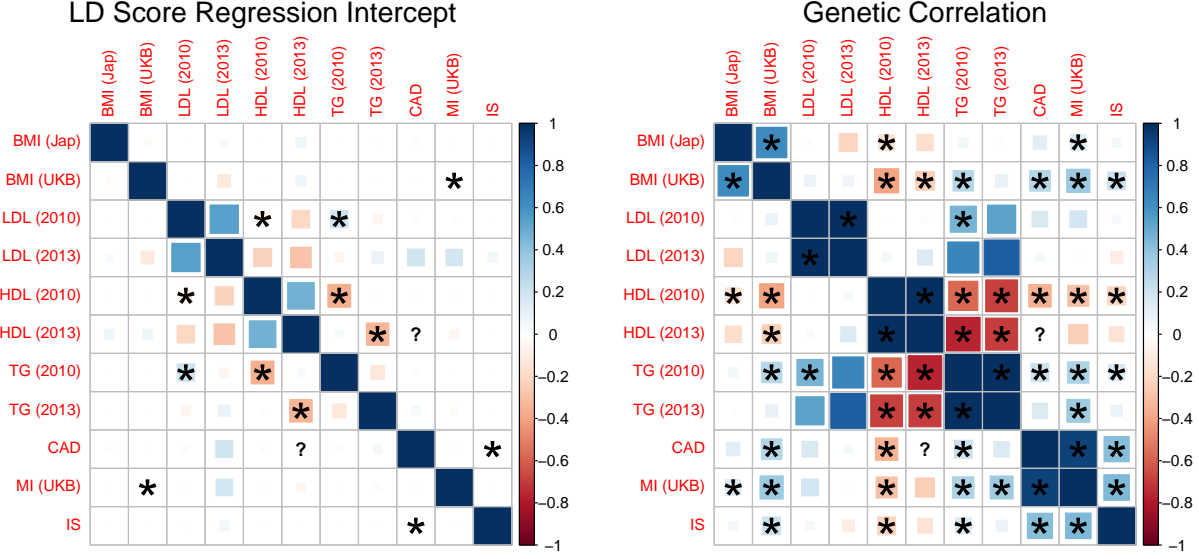


Figure 2: Results of LD score regression for the GWAS datasets. Significant intercepts and slopes (adjusted for multiple testing) are indicated by asterisks.

(No Outlier), ALL (All SNPs), STR (Strong SNPs), WKS (Weak SNPs), NUL (null causal effect), and EXP (exponentially distributed γ). The true causal effect β is set to 0.2 in all settings beside NUL (where $\beta = 0$). This is smaller than the estimated causal effect of LDL-C so that the statistical power is not always 100%. Except for EXP, the effect sizes γ_j/σ_{X_j} , $j = 1, \dots, p$ are generated from the Gaussian mixture distribution with

Settings NOO, ALL, NUL $p = 898$, $p_1 = 0.92$, $\sigma_1 = 0.47$, $\sigma_2 = 3.48$, resembling the analysis of LDL-C using all the 898 SNPs.

Setting STR $p = 11$, $p_1 = 0.01$, $\sigma_1 = \sigma_2 = 5.93$, resembling the analysis using the 11 SNPs that are genome-wide significant in the `selection` dataset.

Setting WKS $p = 887$, $p_1 = 0.92$, $\sigma_1 = 0.44$, $\sigma_2 = 2.39$, resembling the analysis using the 887 SNPs that are not significant in the `selection` dataset.

In setting EXP, the effect sizes are generated from the Laplace distribution with rate 1.5 (i.e. mean absolute value is $2/3$).

Next, $\mathbf{\Gamma}$ is generated by $\Gamma_j = \beta\gamma_j + \alpha_j$ where α_j is an independent Gaussian variable with mean 0 and variance 3.8×10^{-5} , the estimated τ^2 in the LDL-CAD study using all 898 SNPs. In settings ALL, STR, and WKS, we include an outlier (subtract 5τ from the α_j corresponding to the strongest SNP) to test the method's robustness to large idiosyncratic pleiotropy. Finally, the

standard deviations (σ_{Xj}, σ_{Yj}) are the same as the standard errors in the analysis of LDL-C.

Setting (# SNPs, Outlier)	Metric	Method				
		MR-Egger	MR-Egger (SIMEX)	Wtd. Med.	RAPS (MLE)	RAPS (Shrinkage)
NOO (898 SNPs, 0 outlier)	Mean	0.13	0.15	0.12	0.20	0.20
	RMSE	0.088	0.073	0.095	0.073	0.063
	Coverage	61.1%	80.0%	74.2%	94.4%	95.3%
	Power	78.6%	86.2%	56.3%	80.2%	88.9%
ALL (898 SNPs, 1 outlier)	Mean	0.11	0.13	0.10	0.18	0.17
	RMSE	0.105	0.089	0.117	0.082	0.073
	Coverage	47.4%	65.8%	60.2%	91.8%	90.7%
	Power	64.8%	74.9%	40.2%	71.1%	79.1%
STR (11 SNPs, 1 outlier)	Mean	0.08	0.09	0.11	0.12	0.12
	RMSE	0.237	0.163	0.167	0.144	0.145
	Coverage	85.9%	81.1%	81.4%	84.9%	84.7%
	Power	12.2%	20.5%	27.3%	26.0%	26.0%
WKS (887 SNPs, 1 outlier)	Mean	0.08	0.10	0.07	0.18	0.17
	RMSE	0.134	0.116	0.144	0.119	0.106
	Coverage	38.3%	57.6%	50.6%	94.1%	92.6%
	Power	33.6%	46.4%	19.1%	39.4%	44.9%
NUL (898 SNPs, 0 outlier)	Mean	0.00	0.00	0.00	0.00	-0.00
	RMSE	0.045	0.053	0.054	0.074	0.065
	Coverage	93.7%	92.5%	95.9%	93.6%	94.1%
	Power	6.3%	7.5%	4.1%	6.4%	5.9%
EXP (898 SNPs, 0 outlier)	Mean	0.10	0.11	0.08	0.20	0.20
	RMSE	0.112	0.111	0.135	0.085	0.082
	Coverage	50.7%	65.7%	45.8%	94.3%	95.2%
	Power	54.7%	50.7%	22.4%	69.9%	70.5%

Table 2: Simulation results using 1000 replications in 6 settings: NOO (no outlier), ALL (all SNPs), STR (strong SNPs), WKS (weak SNPs), NUL (null causal effect), EXP (exponentially distributed effect sizes). For each estimator we report four metrics: mean of $\hat{\beta}$ (the true $\beta = 0$ in scenario NUL and $\beta = 0.2$ in all other cases), root-mean-squared error (RMSE), coverage of the 95% CI, and statistical power (proportion of 95% CI not covering 0).

Table 2 shows the results of this simulation study for five estimators: MR-Egger [41], MR-Egger with SIMEX correction [56], weighted median [24], RAPS with MLE weights, and RAPS with shrinkage weights (both RAPS estimator use the Huber score function as ψ). In settings with no outlier (NOO, NUL, EXP), the RAPS estimators are unbiased and have the correct confidence interval coverage. This shows that our empirical partially Bayes approach remains unbiased even if the effect size distributions are misspecified. The SIMEX correction helps to reduce the weak

	$p_{\text{sel}} \in (0, 1)$		$p_{\text{sel}} \in (0, 5 \times 10^{-8})$		$p_{\text{sel}} \in (5 \times 10^{-8}, 1)$	
# SNPs	1650		5		1645	
p_1	0.99		0.01		0.88	
σ_1	0.44		1.58		0.25	
σ_2	4.5		6.96		1.25	
MR-Egger	0.353 (0.033)		0.744 (0.476)		0.274 (0.034)	
MR-Egger (SIMEX)	0.744 (0.054)		0.764 (0.559)		0.592 (0.057)	
Wtd. Med.	0.127 (0.035)		0.664 (0.125)		0.089 (0.034)	
	MLE	Shrinkage	MLE	Shrinkage	MLE	Shrinkage
$\tau^2 = 0, \psi_I$	1.029 (0.081)	1.042 (0.076)	0.937 (0.098)	0.936 (0.098)	1.058 (0.106)	1.147 (0.104)
$\tau^2 = 0, \psi_H$	1.058 (0.085)	1.097 (0.08)	0.822 (0.096)	0.821 (0.096)	1.076 (0.112)	1.178 (0.109)
$\tau^2 \neq 0, \psi_I$	1.029 (0.081)	1.042 (0.076)	0.952 (0.178)	0.952 (0.178)	1.058 (0.106)	1.147 (0.104)
$\tau^2 \neq 0, \psi_H$	1.055 (0.133)	1.096 (0.107)	0.926 (0.193)	0.926 (0.193)	1.076 (0.112)	1.178 (0.109)

Table 3: Validation CAD-CAD study: both the exposure and the outcome are coronary artery disease, so the true β should be about 1. Our estimators are roughly unbiased and the shrinkage estimator is about 10% more efficient when all SNPs are used.

instrument bias of MR-Egger but does not completely eliminate it. In other settings with a large outlier (ALL, STR, WKS), the two RAPS estimators have much smaller bias and are generally much more precise than the other methods. Among the two RAPS estimator, the one with shrinkage weights is about 7.5% more efficient in setting EXP and about 25% more efficient in settings NOO, ALL and WKS where the “spike” and the “slab” have greater disparity.

6.2 CAD-CAD study

Our second validation study uses a design in our previous article [20] where the “causal effect” β can be regarded as known. In this example, all three datasets—**selection**, **exposure**, **outcome** (as explained in Section 2)—are GWAS of coronary artery disease. In particular, MI (UKB) is used to select SNPs, while C4D and CARDIoGRAM are used as the exposure and outcome datasets. Since the exposure and outcome are the same variable, it is expected that γ and Γ in our model are the same (or almost equal). Thus $\beta \approx 1$ and $\tau^2 \approx 0$.

In Table 3 we apply our statistical methods to this validation dataset in three ways: using all the SNPs, using SNPs that are genome-wide significant in MI (UKB) ($p\text{-value} \leq 5 \times 10^{-8}$), and using SNPs that are not genome-wide significant in MI (UKB). In all cases the RAPS point estimates are close to the truth $\beta = 1$. When only the strong instruments are used so there is virtually no shrinkage, the shrinkage estimators are essentially the same as the non-shrinkage estimators. When all the SNPs are used, the shrinkage estimators are about 10% more efficient. MR-Egger and

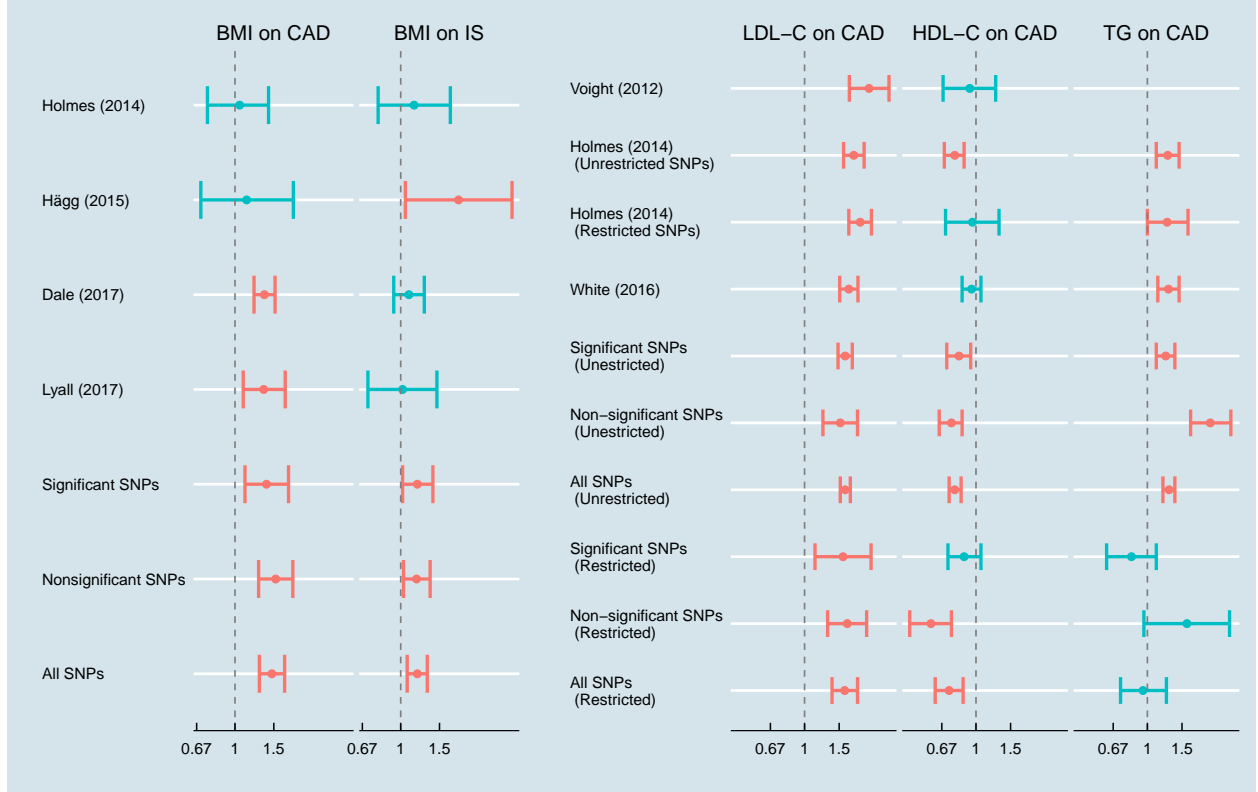


Figure 3: Overview of the MR results for the effect of BMI and blood lipids on cardiovascular diseases.

weighted median are heavily biased by the weak instruments in the CAD-CAD study. The SIMEX correction [56] reduces but does not eliminate the bias of MR-Egger.

7 Application to the effect of BMI and blood lipids on cardiovascular diseases

We apply our method to estimate the causal effect of BMI and blood lipids on cardiovascular disease outcomes. Figure 3 summarizes the main results and Tables 4 and 5 contain more details. By default, we use the RAPS estimator with shrinkage weights, overdispersion adjustment and Huber’s score function. In Tables C1 to C5 in the Appendix, we report the results using different sets of instruments and different MR methods (including different specifications of our RAPS estimator).

7.1 Body Mass Index (BMI)

For the BMI studies we use the BMI (Jap) to select instruments and the BMI (UKB) to obtain the SNP-exposure effects. We consider two outcomes, coronary artery disease (CAD) and ischemic stroke (IS), using two GWAS summary datasets, CAD and IS, as described in Table 1. The results

		Outcome: CAD	Outcome: IS
Previous MR studies for BMI			
Holmes et al. (2014) [30]* (14 SNPs)		1.05 (0.75, 1.42)	1.15 (0.79, 1.68)
Hägg et al. (2015) [31] (32 SNPs)		1.13 (0.70, 1.84)	1.83 (1.05, 3.20)
Dale et al. (2017) [32] (97 SNPs)		1.36 (1.22, 1.52)	1.09 (0.93, 1.28)
Lyll et al. (2017) [33] (93 SNPs)		1.35 (1.09, 1.69)	1.02 (0.71, 1.46)
New MR analysis for BMI			
MR-RAPS	Using 44 significant SNPs	1.39 (1.11, 1.75)	1.19 (1.02, 1.4)
	Using 1075 non-significant SNPs	1.53 (1.28, 1.83)	1.18 (1.03, 1.36)
	Using all 1119 SNPs	1.47 (1.29, 1.68)	1.19 (1.07, 1.32)
	<i>p</i> -value for heterogeneity	0.79	0.78
MR-Egger	Using 44 significant SNPs	1.67 (1.16, 2.40)	1.21 (0.95, 1.54)
	Using 1075 non-significant SNPs	1.56 (1.27, 1.91)	1.11 (0.95, 1.28)
	Using all 1119 SNPs	1.47 (1.26, 1.71)	1.14 (1.02, 1.27)
Wtd. Med.	Using 44 significant SNPs	1.32 (1.02, 1.70)	1.12 (0.91, 1.38)
	Using 1075 non-significant SNPs	1.42 (1.15, 1.75)	1.23 (1.03, 1.46)
	Using all 1119 SNPs	1.33 (1.09, 1.62)	1.12 (0.94, 1.32)

Table 4: Previous and new results of the effect of Body Mass Index (BMI) on coronary artery disease. **Statistically non-significant results are shown in blue color.**

* The original results were reported per 1 kg/m² of increase in BMI. We transformed the results to per 1 SD increase of BMI using $SD(BMI) = 4.6 \text{ kg/m}^2$.

of the BMI studies are reported in Table 4. In summary we find strong evidence that BMI causally increases the risk of CAD and IS and the estimated effects remain stable regardless of the instrument strength. For CAD, in our most powerful analysis using all the instruments, the estimated odds ratio is 1.47 (95% CI 1.29–1.68, p -value $< 10^{-7}$). Using the non-significant SNPs reduces the length of the CI by about 40%. For IS, the corresponding result is 1.19 (95% CI 1.07–1.32, p -value = 0.0008), which is much more precise than the results of previous MR studies.

7.2 Blood lipids

For the lipid studies we use the 2010 GWAS reported by Teslovich et al. [50] to select instruments and the 2013 GWAS (Metabochip data only) by the Global Lipids Genetics Consortium [51]. We use two independent datasets, CAD and MI (UKB), to examine if the MR results replicate in two studies. Because many SNPs are associated with more than one lipid traits, we also consider the restricted sets of instruments that are not associated with the exposure being studied. For

example, a restricted IV for HDL-C must be unassociated with LDL-C and TG (p -value > 0.5 in the **screening dataset**). Our results for the blood lipids are reported in Table 5.

Similar to BMI, the results for LDL-C are highly significant and stable across different datasets and sets of instruments. For CAD, in our most accurate result using all the unrestricted instruments, the estimated odds ratio is 1.61 (95% CI 1.52–1.71). The CI is much shorter than previous MR studies. The estimated odds ratio does not move by much when we use the restricted instruments: 1.6 (95% CI 1.38–1.86), though the CI becomes wider because fewer SNPs are used. Similar observations are found when MI (UKB) is used as the outcome.

For HDL-C, the MR analyses using all the SNPs appears to suggest that HDL-C is protective. For example, in the analysis using the CAD dataset and all the unrestricted instruments, the estimated odds ratio is 0.78 (95% CI 0.73–0.84). However, this highly significant result is mostly driven by the weaker instruments. When using the SNPs that are not genome-wide significant in HDL (2010) dataset, the estimated causal effect becomes weaker and not statistically significant when using the restricted instruments or the MI (UKB) data. The diagnostic plots (Figures C2b, C3b, C4b and C5b) also show strong evidence of heterogeneity between the strong and weak instruments.

For TG, the MR analyses using unrestricted instruments all yield statistically significant results. When using the CAD dataset and all the unrestricted instruments, the estimated odds ratio is 1.29 (95% CI 1.2–1.38). However, our heterogeneity test shows strong evidence of heterogeneity. When using the restricted instruments for both studies, the confidence intervals become very wide and not statistically significant due to the lack of instruments that are exclusively associated with TG. In conclusion, the potential causal role of triglycerides in CAD remains uncertain based on our results.

8 Discussion

Our examples in Sections 6 and 7 demonstrate that a genome-wide MR design is usually much more powerful than a MR analysis that just uses a small set of strong genetic instruments. The empirical partially Bayes technique introduced in this paper can further increase the statistical power.

Our empirical results reaffirm the causal effect of adiposity and LDL-C on the risk of coronary artery disease. Additionally, our MR analysis gives strong support for the causal role of adiposity in the development of ischemic stroke. Another observation is that in these cases the estimated

	Exposure: LDL-c	Exposure: HDL-c	Exposure: TG
Observational studies			
Angelantonio et al. (2009) [57]			
<i>Adjust for non-lipid factors</i>	1.56 (1.47, 1.66)	0.71 (0.68, 0.75)	1.37 (1.31, 1.42)
<i>Also adjust for lipids</i>	1.50 (1.39, 1.61)	0.78 (0.74, 0.82)	0.99 (0.94, 1.05)
Voight et al. (2012) [13]	1.54 (1.45, 1.63)	0.62 (0.58, 0.66)	1.42 (1.31, 1.52)
Previous MR studies			
Voight et al. (2012) [13]	2.13 (1.69, 2.69)	0.93 (0.68, 1.26)	Not reported
Holmes et al. (2014) [14]*			
<i>Unrestricted instruments</i>	1.78 (1.58, 2.01)	0.78 (0.69, 0.87)	1.27 (1.11, 1.45)
<i>Restricted instruments (p > 0.01)</i>	1.92 (1.68, 2.19)	0.96 (0.70, 1.31)	1.26 (1.00, 1.61)
White et al. (2016) [58]			
<i>MR-Egger</i>	1.68 (1.51, 1.87)	0.95 (0.85, 1.06)	1.28 (1.13, 1.45)
<i>Multivariable MR</i>	1.50 (1.39, 1.63)	0.86 (0.78, 0.96)	1.38 (1.19, 1.59)
New MR analysis: Lipids-CAD (CARDIoGRAMplusC4D)			
<i>Unrestricted instruments</i>			
Using significant SNPs	1.61 (1.48, 1.75)	0.82 (0.71, 0.94)	1.24 (1.11, 1.38)
Using non-significant SNPs	1.52 (1.24, 1.86)	0.75 (0.65, 0.85)	2.09 (1.66, 2.66)
Using all SNPs	1.61 (1.52, 1.71)	0.78 (0.73, 0.84)	1.29 (1.2, 1.38)
p-value for heterogeneity	0.21	< 0.001	< 0.001
<i>Restricted instruments (p > 0.5)</i>			
Using significant SNPs	1.57 (1.13, 2.18)	0.87 (0.72, 1.06)	0.83 (0.62, 1.11)
Using non-significant SNPs	1.65 (1.31, 2.07)	0.59 (0.46, 0.75)	1.59 (0.96, 2.62)
Using all SNPs	1.6 (1.38, 1.86)	0.73 (0.62, 0.86)	0.95 (0.73, 1.25)
p-value for heterogeneity	0.08	0.36	0.19
New MR analysis: Lipids-MI (UK BioBank)			
<i>Unrestricted instruments</i>			
Using significant SNPs	1.27% (1.04%, 1.49%)	-0.43% (-0.96%, 0.10%)	0.72% (0.32%, 1.12%)
Using non-significant SNPs	1.06% (0.39%, 1.72%)	-1.07% (-1.54%, -0.60%)	2.41% (1.61%, 3.21%)
Using all SNPs	1.24% (1.03%, 1.45%)	-0.77% (-1.02%, -0.53%)	1.03% (0.77%, 1.28%)
p-value for heterogeneity	0.99	< 0.001	< 0.001
<i>Restricted instruments (p > 0.5)</i>			
Using significant SNPs	1.37% (0.25%, 2.49%)	-0.25% (-1.04%, 0.53%)	0.36% (-0.77%, 1.49%)
Using non-significant SNPs	1.49% (0.53%, 2.45%)	-2.26% (-3.14%, -1.37%)	1.7% (-0.61%, 4.00%)
Using all SNPs	1.25% (0.63%, 1.88%)	-1.28% (-1.88%, -0.67%)	0.51% (-0.55%, 1.57%)
p-value for heterogeneity	0.66	0.1	0.06

Table 5: Previous and new results of the effect of major blood lipids on coronary artery disease (or myocardial infarction) risk. The numbers reported in the Angelantonio et al. (2009) study are hazard ratios, and the numbers reported in the new MR analysis using UK BioBank are risk differences. All other numbers are odds ratios. The prevalence of myocardial infarction in UK BioBank is $8288/360420 = 2.30\%$, so a risk difference of 1% roughly corresponds to an odds ratio of 1.45. **Statistically non-significant results are shown in blue color.**

* The original results for the Holmes et al. (2014 study) were reported per 1 mmol/L increase of LDL-c and HDL-c and 1 log unit increase of TG. We transformed the results to per 1 SD increase using the following approximate standard deviations: $SD(\text{LDL-c}) = 1 \text{ mmol/L}$, $SD(\text{HDL-c}) = 0.4 \text{ mmol/L}$, $SD(\text{Log TG}) = 0.5$.

causal effects are very close across different strength of the instruments. The homogeneity of the effect further adds evidence to these causal relationships.

In comparison, although our most powerful genome-wide MR analyses show that the effect of HDL-C on CAD is highly significant, there is also strong evidence of effect heterogeneity. Indeed, the statistical significance is mostly driven by the weak instruments. When used alone, the weak instruments give very different effect estimates (with non-overlapping confidence intervals) than the strong instruments. The role of HDL-C in cardiovascular disease has been heatedly debated in the recent years following the failure of several highly anticipated clinical trials for the *CETP* inhibitors [59, 60, 61]. Observational epidemiology studies have long suggested that HDL-C is inversely associated with the risk of myocardial infarction [57, 62, 63]. However, the failed *CETP* trials and previous MR studies [13, 30] have led to the broad conclusion that HDL-C is unlikely a causal agent for atherosclerotic cardiovascular disease [64, 65], though some remain hopeful in the HDL function hypothesis [65, 66, 67]. Our MR analyses suggest that the causal role of HDL-C remains uncertain and the effect of HDL-C is heterogeneous using different instruments. Relatedly, Bulik-Sullivan et al. (2015) [21] also observed statistical significant genetic correlation (computed across the whole genome) between HDL-C and CAD (see also Figure 2). We think further investigations are needed to demystify the strong observational and genetic associations between HDL-C and CAD.

References

- [1] Davey Smith G, Hemani G. Mendelian randomization: genetic anchors for causal inference in epidemiological studies. *Human Molecular Genetics*. 2014;23(R1):R89–R98.
- [2] Linsel-Nitschke P, Götz A, Erdmann J, Braenne I, Braund P, Hengstenberg C, et al. Life-long reduction of LDL-cholesterol related to a common variant in the LDL-receptor gene decreases the risk of coronary artery disease—a Mendelian Randomisation study. *PloS ONE*. 2008;3(8):e2986.
- [3] Ference BA, Yoo W, Alesh I, Mahajan N, Mirowska KK, Mewada A, et al. Effect of long-term exposure to lower low-density lipoprotein cholesterol beginning early in life on the risk of coronary heart disease: a Mendelian randomization analysis. *Journal of the American College of Cardiology*. 2012;60(25):2631–2639.
- [4] Myocardial Infarction Genetics Consortium Investigators. Inactivating mutations in

- NPC1L1 and protection from coronary heart disease. *New England Journal of Medicine*. 2014;371(22):2072–2082.
- [5] Burgess S, Harshfield E. Mendelian randomization to assess causal effects of blood lipids on coronary heart disease: lessons from the past and applications to the future. *Current Opinion in Endocrinology, Diabetes, and Obesity*. 2016;23(2):124.
 - [6] Scandinavian Simvastatin Survival Study Group. Randomised trial of cholesterol lowering in 4444 patients with coronary heart disease: the Scandinavian Simvastatin Survival Study (4S). *Lancet*. 1994;344(8934):1383–1389.
 - [7] Hernán MA, Robins JM. Instruments for causal inference: an epidemiologist’s dream? *Epidemiology*. 2006;17(4):360–372.
 - [8] Didelez V, Sheehan N. Mendelian randomization as an instrumental variable approach to causal inference. *Statistical Methods in Medical Research*. 2007;16(4):309–330.
 - [9] Angrist JD, Krueger AB. Does compulsory school attendance affect schooling and earnings? *Quarterly Journal of Economics*. 1991;106(4):979–1014.
 - [10] Baiocchi M, Cheng J, Small DS. Instrumental variable methods for causal inference. *Statistics in Medicine*. 2014;33(13):2297–2340.
 - [11] Solovieff N, Cotsapas C, Lee PH, Purcell SM, Smoller JW. Pleiotropy in complex traits: challenges and strategies. *Nature Reviews Genetics*. 2013;14(7):483–495.
 - [12] Verbanck M, Chen CY, Neale B, Do R. Detection of widespread horizontal pleiotropy in causal relationships inferred from Mendelian randomization between complex traits and diseases. *Nature Genetics*. 2018;50:693–698.
 - [13] Voight BF, Peloso GM, Orho-Melander M, Frikke-Schmidt R, Barbalic M, Jensen MK, et al. Plasma HDL cholesterol and risk of myocardial infarction: a mendelian randomisation study. *Lancet*. 2012;380(9841):572–580.
 - [14] Holmes MV, Asselbergs FW, Palmer TM, Drenos F, Lanktree MB, Nelson CP, et al. Mendelian randomization of blood lipids for coronary heart disease. *European Heart Journal*. 2014;36(9):539–550.

- [15] Hemani G, Zheng J, Wade KH, Laurin C, Elsworth B, Burgess S, et al. MR-Base: a platform for systematic causal inference across the phenome using billions of genetic associations. *bioRxiv:078972*. 2016;.
- [16] Katan M. Apolipoprotein E isoforms, serum cholesterol, and cancer. *Lancet*. 1986;327(8479):507–508.
- [17] Davey Smith G, Ebrahim S. "Mendelian randomization": can genetic epidemiology contribute to understanding environmental determinants of disease? *International Journal of Epidemiology*. 2003;32(1):1–22.
- [18] Stock JH, Wright JH, Yogo M. A survey of weak instruments and weak identification in generalized method of moments. *Journal of Business & Economic Statistics*. 2002;20(4):518–529.
- [19] Hansen C, Hausman J, Newey W. Estimation with many instrumental variables. *Journal of Business and Economic Statistics*. 2008;26(4):398–422.
- [20] Zhao Q, Wang J, Hemani G, Bowden J, Small DS. Statistical inference in two-sample summary-data Mendelian randomization using robust adjusted profile score. *arXiv preprint arXiv:180109652*. 2018;.
- [21] Bulik-Sullivan B, Finucane HK, Anttila V, Gusev A, Day FR, Loh PR, et al. An atlas of genetic correlations across human diseases and traits. *Nature Genetics*. 2015;47(11):1236.
- [22] Bowden J, Fabiola Del Greco M, Minelli C, Lawlor D, Zhao Q, Sheehan N, et al. Improving the accuracy of two-sample summary data Mendelian randomization: moving beyond the NOME assumption. *International Journal of Epidemiology*. 2018;to appear.
- [23] Kang H, Zhang A, Cai TT, Small DS. Instrumental variables estimation with some invalid instruments and its application to Mendelian randomization. *Journal of American Statistical Association*. 2016;111(513):132–144.
- [24] Bowden J, Davey Smith G, Haycock PC, Burgess S. Consistent estimation in Mendelian randomization with some invalid instruments using a weighted median estimator. *Genetic Epidemiology*. 2016;40(4):304–314.

- [25] Guo Z, Kang H, Cai TT, Small DS. Confidence intervals for causal effects with invalid instruments using two-stage hard thresholding with voting. *Journal of the Royal Statistical Society Series B (Methodological)*. 2018;to appear.
- [26] Evans DM, Brion MJA, Paternoster L, Kemp JP, McMahon G, Munafò M, et al. Mining the human phenome using allelic scores that index biological intermediates. *PLoS genetics*. 2013;9(10):e1003919.
- [27] Brion MJA, Benyamin B, Visscher PM, Smith GD. Beyond the single SNP: emerging developments in Mendelian randomization in the "Omics" era. *Current Epidemiology Reports*. 2014;1(4):228–236.
- [28] Evans DM, Davey Smith G. Mendelian randomization: new applications in the coming age of hypothesis-free causality. *Annual Review of Genomics and Human Genetics*. 2015;16:327–350.
- [29] Lindsay BG. Using empirical partially Bayes inference for increased efficiency. *Annals of Statistics*. 1985;13(3):914–931.
- [30] Holmes MV, Lange LA, Palmer T, Lanktree MB, North KE, Almoguera B, et al. Causal effects of body mass index on cardiometabolic traits and events: a Mendelian randomization analysis. *American Journal of Human Genetics*. 2014;94(2):198–208.
- [31] Hägg S, Fall T, Ploner A, Mägi R, Fischer K, Draisma HH, et al. Adiposity as a cause of cardiovascular disease: a Mendelian randomization study. *International Journal of Epidemiology*. 2015;44(2):578–586.
- [32] Dale CE, Fatemifar G, Palmer TM, White J, Prieto-Merino D, Zabaneh D, et al. Causal associations of adiposity and body fat distribution with coronary heart disease, stroke subtypes, and type 2 diabetes mellitus: a Mendelian randomization analysis. *Circulation*. 2017;135(24):2373–2388.
- [33] Lyall DM, Celis-Morales C, Ward J, Iliodromiti S, Anderson JJ, Gill JM, et al. Association of body mass index with cardiometabolic disease in the UK Biobank: a Mendelian randomization study. *JAMA cardiology*. 2017;2(8):882–889.
- [34] Akiyama M, Okada Y, Kanai M, Takahashi A, Momozawa Y, Ikeda M, et al. Genome-wide association study identifies 112 new loci for body mass index in the Japanese population. *Nature Genetics*. 2017;49(10):1458.

- [35] Abbott L, Bryant S, Churchhouse C, Ganna A, Howrigan D, Palmer D, et al.. Round 2 GWAS results of thousands of phenotype in the UK BioBank; 2018. Available from: <http://www.nealelab.is/uk-biobank/>.
- [36] The CARDIoGRAMplusC4D Consortium, Nikpay M, Goel A, Won HH, Hall LM, Willenborg C, et al. A comprehensive 1000 Genomes-based genome-wide association meta-analysis of coronary artery disease. *Nature Genetics*. 2015;47(10):1121.
- [37] Purcell S, Neale B, Todd-Brown K, Thomas L, Ferreira MA, Bender D, et al. PLINK: a tool set for whole-genome association and population-based linkage analyses. *American Journal of Human Genetics*. 2007;81(3):559–575.
- [38] Burgess S, Scott RA, Timpson NJ, Smith GD, Thompson SG, Consortium EI. Using published data in Mendelian randomization: a blueprint for efficient identification of causal risk factors. *European Journal of Epidemiology*. 2015;30(7):543–552.
- [39] Burgess S, Thompson SG, Collaboration CCG. Avoiding bias from weak instruments in Mendelian randomization studies. *International Journal of Epidemiology*. 2011;40(3):755–764.
- [40] Bowden J, Del Greco M, Minelli C, Davey Smith G, Sheehan N, Thompson J. A framework for the investigation of pleiotropy in two-sample summary data Mendelian randomization. *Statistics in Medicine*. 2017;36(11):1783–1802.
- [41] Bowden J, Davey Smith G, Burgess S. Mendelian randomization with invalid instruments: effect estimation and bias detection through Egger regression. *International Journal of Epidemiology*. 2015;44(2):512–525.
- [42] Burgess S, Thompson SG. Multivariable Mendelian randomization: the use of pleiotropic genetic variants to estimate causal effects. *American Journal of Epidemiology*. 2015;181(4):251–260.
- [43] Sanderson E, Smith GD, Windmeijer F, Bowden J. An examination of multivariable Mendelian randomization in the single sample and two-sample summary data settings. *bioRxiv*. 2018;p. 306209.
- [44] Mitchell TJ, Beauchamp JJ. Bayesian variable selection in linear regression. *Journal of American Statistical Association*. 1988;83(404):1023–1032.

- [45] George EI, McCulloch RE. Variable selection via Gibbs sampling. *Journal of American Statistical Association*. 1993;88(423):881–889.
- [46] Ishwaran H, Rao JS. Spike and slab variable selection: frequentist and Bayesian strategies. *Annals of Statistics*. 2005;33(2):730–773.
- [47] Neyman J, Scott EL. Consistent estimates based on partially consistent observations. *Econometrica*. 1948;16(1):1–32.
- [48] Jordan DM, Verbanck M, Do R. The landscape of pervasive horizontal pleiotropy in human genetic variation is driven by extreme polygenicity of human traits and diseases. *bioRxiv*. 2018;p. 311332.
- [49] Bowden J, Spiller W, Del Greco M F, Sheehan N, Thompson J, Minelli C, et al. Improving the visualization, interpretation and analysis of two-sample summary data Mendelian randomization via the Radial plot and Radial regression. *International Journal of Epidemiology*. 2018;47(4):1264–1278.
- [50] Teslovich TM, Musunuru K, Smith AV, Edmondson AC, Stylianou IM, Koseki M, et al. Biological, clinical and population relevance of 95 loci for blood lipids. *Nature*. 2010;466(7307):707.
- [51] Global Lipids Genetics Consortium. Discovery and refinement of loci associated with lipid levels. *Nature Genetics*. 2013;45(11):1274.
- [52] Schunkert H, König IR, Kathiresan S, Reilly MP, Assimes TL, Holm H, et al. Large-scale association analysis identifies 13 new susceptibility loci for coronary artery disease. *Nature Genetics*. 2011;43(4):333.
- [53] Coronary Artery Disease (C4D) Genetics Consortium, et al. A genome-wide association study in Europeans and South Asians identifies five new loci for coronary artery disease. *Nature Genetics*. 2011;43(4):339.
- [54] Malik R, Chauhan G, Traylor M, Sargurupremraj M, Okada Y, Mishra A, et al. Multiancestry genome-wide association study of 520,000 subjects identifies 32 loci associated with stroke and stroke subtypes. *Nature Genetics*. 2018;50(4):524.
- [55] Bulik-Sullivan BK, Loh PR, Finucane HK, Ripke S, Yang J, Patterson N, et al. LD score

- regression distinguishes confounding from polygenicity in genome-wide association studies. *Nature Genetics*. 2015;47(3):291.
- [56] Bowden J, Del Greco M F, Minelli C, Davey Smith G, Sheehan NA, Thompson JR. Assessing the suitability of summary data for two-sample Mendelian randomization analyses using MR-Egger regression: the role of the I^2 statistic. *International Journal of Epidemiology*. 2016;45(6):1961–1974.
- [57] Emerging Risk Factors Collaboration. Major lipids, apolipoproteins, and risk of vascular disease. *JAMA*. 2009;302(18):1993–2000.
- [58] White J, Swerdlow DI, Preiss D, Fairhurst-Hunter Z, Keating BJ, Asselbergs FW, et al. Association of lipid fractions with risks for coronary artery disease and diabetes. *JAMA Cardiology*. 2016;1(6):692–699.
- [59] Barter PJ, Caulfield M, Eriksson M, Grundy SM, Kastelein JJ, Komajda M, et al. Effects of torcetrapib in patients at high risk for coronary events. *New England Journal of Medicine*. 2007;357(21):2109–2122.
- [60] Schwartz GG, Olsson AG, Abt M, Ballantyne CM, Barter PJ, Brumm J, et al. Effects of dalcetrapib in patients with a recent acute coronary syndrome. *New England Journal of Medicine*. 2012;367(22):2089–2099.
- [61] Lincoff AM, Nicholls SJ, Riesmeyer JS, Barter PJ, Brewer HB, Fox KA, et al. Evacetrapib and cardiovascular outcomes in high-risk vascular disease. *New England Journal of Medicine*. 2017;376(20):1933–1942.
- [62] Miller GJ, Miller NE. Plasma-high-density-lipoprotein concentration and development of ischaemic heart-disease. *Lancet*. 1975;305(7897):16–19.
- [63] Prospective Studies Collaboration. Blood cholesterol and vascular mortality by age, sex, and blood pressure: a meta-analysis of individual data from 61 prospective studies with 55,000 vascular deaths. *Lancet*. 2007;370(9602):1829–1839.
- [64] Holmes MV, Ala-Korpela M, Smith GD. Mendelian randomization in cardiometabolic disease: challenges in evaluating causality. *Nature Reviews Cardiology*. 2017;14(10):577.

- [65] Rosenson RS, Brewer Jr HB, Barter PJ, Björkegren JL, Chapman MJ, Gaudet D, et al. HDL and atherosclerotic cardiovascular disease: genetic insights into complex biology. *Nature Reviews Cardiology*. 2018;15(1):9.
- [66] Rader DJ, Hovingh GK. HDL and cardiovascular disease. *Lancet*. 2014;384(9943):618–625.
- [67] Rohatgi A, Khera A, Berry JD, Givens EG, Ayers CR, Wedin KE, et al. HDL cholesterol efflux capacity and incident cardiovascular events. *New England Journal of Medicine*. 2014;371(25):2383–2393.
- [68] Kiefer J, Wolfowitz J. Consistency of the maximum likelihood estimator in the presence of infinitely many incidental parameters. *Annals of Mathematical Statistics*. 1956;27(4):887–906.
- [69] Feng L, Dicker LH. Approximate nonparametric maximum likelihood for mixture models: A convex optimization approach to fitting arbitrary multivariate mixing distributions. *Computational Statistics & Data Analysis*. 2018;122:80–91.
- [70] Cox D. A note on partially Bayes inference and the linear model. *Biometrika*. 1975;62(3):651–654.
- [71] Meng XL. Automated bias-variance trade-off: intuitive inadmissibility or inadmissible intuition. In: Chen MH, Müller P, Sun D, Ye K, Dey DK, editors. *Frontiers of Statistical Decision Making and Bayesian Analysis*. New York: Springer; 2010. .
- [72] Lindsay B. Conditional score functions: some optimality results. *Biometrika*. 1982;69(3):503–512.
- [73] Stefanski LA, Carroll RJ. Conditional scores and optimal scores for generalized linear measurement-error models. *Biometrika*. 1987;74(4):703–716.
- [74] James W, Stein C. Estimation with quadratic loss. In: *Proceedings of the Fourth Berkeley Symposium on Mathematical Statistics and Probability*. vol. 1; 1961. p. 361–379.
- [75] Efron B, Morris C. Stein’s estimation rule and its competitors—an empirical Bayes approach. *Journal of the American Statistical Association*. 1973;68(341):117–130.
- [76] Huber PJ. Robust estimation of a location parameter. *Annals of Mathematical Statistics*. 1964;35(1):73–101.

- [77] Maronna R, Martin RD, Yohai V. Robust Statistics: Theory and Methods. John Wiley & Sons; 2006.

A Technical details

A.1 The empirical partially Bayes approach

We propose a new way of eliminating the nuisance parameters γ that can increase the power of genome-wide MR studies when most IVs are very weak (i.e. γ are very close to 0). The key idea is to view the errors-in-variables regression as a semiparametric problem: instead of treating the vector γ as the nuisance parameter whose dimension grows as more SNPs are used, we treat the (empirical) distribution of γ as the nuisance. This idea originates from the general solution given by Kiefer and Wolfowitz [68] to the Neyman-Scott problem in which the observed data are modeled by a mixture distribution. In principle, the statistical inference can be carried out by solving a nonparametric maximum likelihood problem, but the numerical problem is often extremely challenging [69].

We will take an empirical partially Bayes approach introduced by Lindsay [29] which is numerically feasible and still has several good theoretical properties. The approach is partially Bayes because only the nuisance parameters are modeled by a prior distribution [70, 71]. It is empirical Bayes because the prior distribution is estimated empirically using the observed data.

Consider the simplest scenario where $\alpha = \mathbf{0}$ and derive the conditional score function [72]. When $\alpha = \mathbf{0}$, the log-likelihood function of the data $(\hat{\gamma}, \hat{\Gamma})$ is given by

$$l(\beta, \gamma) = \prod_{j=1}^p l_j(\beta, \gamma_j), \text{ where } l_j(\beta, \gamma_j) = -\frac{(\hat{\gamma}_j - \gamma_j)^2}{2\sigma_{Xj}^2} - \frac{(\hat{\Gamma}_j - \beta\gamma_j)^2}{2\sigma_{Yj}^2}.$$

Thus the score function of β in the j -th SNP is given by

$$S_j(\beta, \gamma_j) = \frac{\partial}{\partial \beta} l_j(\beta, \gamma_j) = \frac{\gamma_j(\hat{\Gamma}_j - \beta\gamma_j)}{\sigma_{Yj}^2}.$$

and a sufficient statistic of the nuisance parameter γ_j is

$$W_j(\beta) = \frac{\hat{\gamma}_j}{\sigma_{Xj}^2} + \frac{\beta\hat{\Gamma}_j}{\sigma_{Yj}^2}. \quad (1)$$

When β is given, the maximum likelihood estimator (MLE) of γ_j is

$$\hat{\gamma}_{j,\text{MLE}}(\beta) = \frac{W_j(\beta)}{1/\sigma_{Xj}^2 + \beta^2/\sigma_{Yj}^2}.$$

The conditional score function is the residual of the score function S_j conditioning on W_j . After

some algebra, we obtain

$$C_j(\beta, \gamma_j) = S_j(\beta, \gamma_j) - \mathbb{E}[S_j(\beta, \gamma_j)|W_j(\beta)] = \frac{\gamma_j(\hat{\Gamma}_j - \beta\hat{\gamma}_j)}{\beta^2\sigma_{X_j}^2 + \sigma_{Y_j}^2}. \quad (2)$$

We would like to make three remarks on the conditional score (2). First, it is proportional to the “regression residual” $\hat{\Gamma}_j - \beta\hat{\gamma}_j$ which has mean 0 at the true β . Second, the nuisance parameter appears in (2) only as a weight to the “regression residual”, as noticed by Lindsay [29]. Third, the sufficient statistic $W_j(\beta)$ of γ_j in (1) is independent of $\hat{\Gamma}_j - \beta\hat{\gamma}_j$ because they are jointly normal and their covariance is 0, regardless of what β is. See [73] for a related application of the conditional score in measurement error models. These observations motivate the following estimating function of β :

$$C(\beta) = \sum_{j=1}^p C_j(\beta, \hat{\gamma}_j(\beta, W_j(\beta))) = \sum_{j=1}^p \frac{\hat{\gamma}_j(\beta, W_j(\beta)) \cdot (\hat{\Gamma}_j - \beta\hat{\gamma}_j)}{\beta^2\sigma_{X_j}^2 + \sigma_{Y_j}^2}, \quad (3)$$

where $\hat{\gamma}_j(\beta, W_j(\beta))$ is any estimator of $\hat{\gamma}_j$ that only depends on the sufficient statistic $W_j(\beta)$, not necessarily the MLE. It is obvious that the estimating function is always unbiased, i.e. $\mathbb{E}[C(\beta)] = 0$ at the true value of β , regardless of what form of $\hat{\gamma}_j$ is used. The estimator $\hat{\beta}$ is obtained by solving $C(\beta) = 0$.

The profile score approach [20] can be viewed as a special case of the conditional score, where the “weights” are the MLE of γ_j : $\hat{\gamma}_j(\beta, W_j(\beta)) = \hat{\gamma}_{j,\text{MLE}}(\beta)$. This is also equivalent to using a flat prior in the partially Bayes approach that will be explained shortly. Under regularity conditions, we prove in our previous article [20] that the profile score provides a consistent and asymptotically normal estimator of β . However, this estimator is not efficient in general. To see this, let’s assume most γ_j are equal to 0. Intuitively, the j -th IV provides no information on β because the distribution of $(\hat{\gamma}_j, \hat{\Gamma}_j)$ does not depend on β . However, some information is still used to estimate γ_j in the MLE, resulting in a loss of statistical efficiency. This phenomenon is particularly relevant in genome-wide MR as most of the genetic instruments are very weak.

When $\sigma_{X_j}^2$ and $\sigma_{Y_j}^2$ are equal across j , Lindsay [29] points out that the efficient estimator of β is given by the weight $\hat{\gamma}_j^* = \mathbb{E}_{\pi^*}[\gamma_j|W_j(\beta)]$, where π^* is the empirical distribution of γ . However, since γ and hence π^* is unknown, it is impossible to compute $\hat{\gamma}_j^*$ directly. Lindsay proposes to use the empirical Bayes (EB) estimator of γ . Suppose the distribution of γ is modeled by a parametric family π_η and $\hat{\eta}$ is an estimate of η using the observed data. We can use

$$\hat{\gamma}_{j,\text{EB}}(\beta, W_j(\beta)) = \mathbb{E}_{\pi_{\hat{\eta}}}[\gamma_j|W_j(\beta)] \quad (4)$$

in the estimating function (3). Since this is usually a better estimator of the whole vector γ than the MLE, a phenomenon known as the James-Stein paradox [74, 75], it is natural to expect that the resulting function of β is also more efficient than the profile score. In fact, Lindsay [29] shows that the estimator has a local efficiency property: when the parametric distribution π_η is specified correctly, the estimator $\hat{\beta}$ is asymptotically efficient; when π_η is specified incorrectly, the estimator is not efficient but still consistent.

A.2 Implementation details

A.2.1 Spike-and-slab prior

Model (4.2) implies that $\hat{\gamma}_j/\sigma_{Xj}$ also follows a Gaussian mixture distribution marginally:

$$\hat{\gamma}_j/\sigma_{Xj} \stackrel{i.i.d.}{\sim} p_1 \cdot N(0, \sigma_1^2 + 1) + (1 - p_1) \cdot N(0, \sigma_2^2 + 1), \quad j = 1, \dots, p. \quad (5)$$

In practice we use maximum likelihood to estimate the prior parameters $(p_1, \sigma_1^2, \sigma_2^2)$ by fitting the marginal mixture model (5) to the exposure z -statistics $\hat{\gamma}_j/\sigma_{Xj}$, $j = 1, \dots, p$.

The posterior mean of γ_i/σ_{Xi} can be computed using the formulas in Proposition 1.

Proposition 1. *Suppose $Z \sim N(\gamma, \sigma^2)$, $\gamma \sim p_1 N(\mu_1, \sigma_1^2) + (1 - p_1) N(\mu_2, \sigma_2^2)$, then $\gamma|Z \sim \tilde{p} \cdot N(\tilde{\mu}_1, \tilde{\sigma}_1^2) + (1 - \tilde{p}) \cdot N(\tilde{\mu}_2, \tilde{\sigma}_2^2)$, where*

$$\tilde{\mu}_k = \frac{Z/\sigma^2 + \mu_k/\sigma_k^2}{1/\sigma^2 + 1/\sigma_k^2}, \quad \tilde{\sigma}_k^2 = \frac{1}{1/\sigma^2 + 1/\sigma_k^2}, \quad \text{and}$$

$$\tilde{p} = \frac{p_1 \cdot \varphi(Z; \mu_1, \sigma^2 + \sigma_1^2)}{p_1 \cdot \varphi(Z; \mu_1, \sigma^2 + \sigma_1^2) + (1 - p_1) \cdot \varphi(Z; \mu_2, \sigma^2 + \sigma_2^2)}.$$

In the above equation, $\varphi(z; \mu, \sigma^2)$ is the probability density function of the normal distribution $N(\mu, \sigma^2)$: $\varphi(z; \mu, \sigma^2) = (\sqrt{2\pi\sigma^2})^{-1} \exp\{-(z - \mu)^2/(2\sigma^2)\}$. The posterior mean of γ is given by $\hat{\gamma} = \mathbb{E}[\gamma|Z] = \tilde{p}\tilde{\mu}_1 + (1 - \tilde{p})\tilde{\mu}_2$.

We want to make two remarks about the choice of prior distribution. First, there is an attractive property of setting the means to be 0 in (4.2). Using Proposition 1, it is easy to verify that, when $\mu_1 = \mu_2 = 0$, $\mathbb{E}[\gamma|Z] = -\mathbb{E}[\gamma] - Z$. As a consequence, the estimating functions in (4.3) are invariant to allele-recoding, meaning if a pair of observations $(\hat{\gamma}_j, \hat{\Gamma}_j)$ is replaced by $(-\hat{\gamma}_j, -\hat{\Gamma}_j)$, the point estimate $\hat{\beta}$ is unchanged. This is desirable because the allele coding used in a GWAS is often arbitrary. The second remark is that the spike-and-slab implementation is actually quite

important in order to gain efficiency. To see this, suppose a single Gaussian prior is used (as in the empirical Bayes interpretation of the James-Stein estimator). It is easy to show that every SNP then receives the same amount of multiplicative shrinkage, so the first estimating function in (4.3) is just scaled by a constant. As a consequence, the estimator $\hat{\beta}$ is the same no matter how large the shrinkage is. By using a spike-and-slab prior, every genetic instrument is shrunk selectively [46] according to its strength and thus efficiency might be gained. It is then natural to expect that the efficiency gain is more substantial when the two components are more distant (σ_1 and σ_2 are more different). See Section 6 for an example.

In Figure A1 we examine the fit of the Gaussian mixture model (5) for our primary analysis of HDL-c in Section 7. In this example we selected 1122 SNPs and the estimated prior parameters are $p_1 = 0.91$, $\sigma_1 = 0.73$, $\sigma_2 = 4.57$. In the left panel of Figure A1 we compare the empirical distribution of $\hat{\gamma}_j/\sigma_{X_j}$ (black histogram) with the fitted Gaussian mixture distribution in (5) (red curve). We find the empirical fit is quite good. In the right panel of Figure A1 we plot the empirical Bayes shrinkage estimator as a function of the z -score. When the z -score is close to 0, it is shrunk aggressively towards 0; when the z -score is large (e.g. greater than 5), there is essentially no shrinkage.

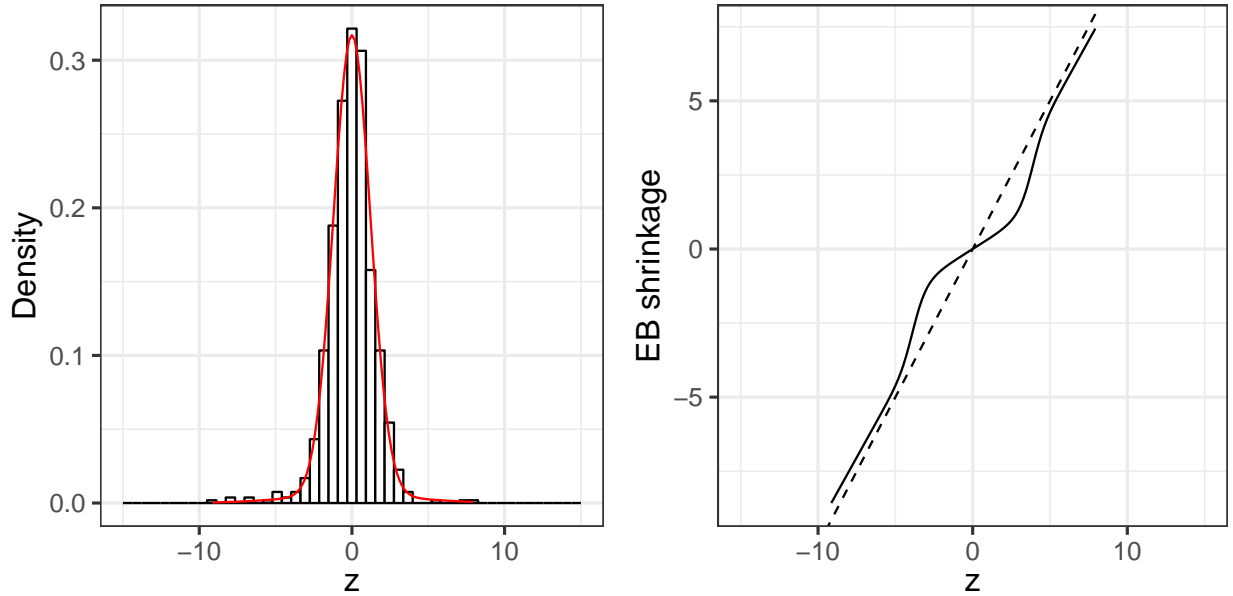


Figure A1: Examine the fitted prior distribution for HDL-C using 861 restricted SNPs used in Table C3b. The left panel compares the empirical distribution of $z_j = \hat{\gamma}_j/\sigma_{X_j}$ (black histogram) with the fitted Gaussian mixture distribution in (5) (red curve). The right panel shows the posterior mean as a function of the z -score.

A.2.2 Choice of robust score function

In our empirical analysis we will consider two choices of the function $\psi(\cdot)$. The first is the identity function $\psi_I(t) = t$ which is non-robust, and the second is the Huber score function [76] that is robust:

$$\psi_H(t) = \begin{cases} t, & \text{if } |t| \leq k, \\ k \cdot \text{sign}(t), & \text{otherwise.} \end{cases}$$

The tuning constant k is chosen to be 1.345, which corresponds to 95% asymptotic efficiency for normal samples in the standard location problem. Another common choice of the robust score function is Tukey's biweight [77], where large outliers essentially have no influence on the estimator. In practice we find that using Tukey's biweight usually gives more local roots than Huber's score. Thus we only report results of the more stable Huber's score in the application.

A.2.3 Multiple roots of the estimating equations

In practice, the estimating functions in (4.3) may have multiple roots. Some roots are trivial: it is straightforward to show that $\tilde{C}(\beta, \tau^2) \rightarrow 0$ if $\beta \rightarrow \pm\infty$ or $\tau^2 \rightarrow \pm\infty$. These unbounded roots can be easily ruled out. However, often there are multiple finite roots. When this happens, we report the root whose $\hat{\beta}$ is closest to the profile-likelihood estimator of β assuming all the SNPs are valid IVs [20]. The latter is always unique because it solves an optimization problem. When there is another root that is also close to the profile-likelihood estimator (the criterion we use in the application is the absolute difference is no more than 5 times the closest difference), we report the empirical partially Bayes estimator is not available.

A.2.4 Standard error of the estimator

Our final problem is to compute the standard error of the estimator $\hat{\theta} = (\hat{\beta}, \hat{\tau}^2)$. For the calculation below we assume all SNPs satisfy $\alpha_j \sim N(0, \tau^2)$, i.e. there is no outlier. After taking a first-order Taylor expansion at the true value of $\theta = (\beta, \tau^2)$,

$$\mathbf{0} = \tilde{C}(\hat{\theta}) \approx \tilde{C}(\theta) + \nabla \tilde{C}(\theta) \cdot (\hat{\theta} - \theta),$$

the variance of $\hat{\boldsymbol{\theta}}$ can be approximated using the Delta method by

$$\text{Var}(\hat{\boldsymbol{\theta}}) \approx \left[\nabla \tilde{\mathbf{C}}(\boldsymbol{\theta}) \right]^{-1} \text{Var} \left(\tilde{\mathbf{C}}(\boldsymbol{\theta}) \right) \left[\nabla \tilde{\mathbf{C}}(\boldsymbol{\theta}) \right]^{-T}.$$

By repeatedly using the fact that $\hat{\gamma}_{j,\text{EB}}$ is independent of $t_j(\beta, \tau^2)$ (so several terms have mean 0 and are dismissed), we obtain, after some algebra, that

$$\begin{aligned} \text{Var} \left(\tilde{\mathbf{C}}(\boldsymbol{\theta}) \right) &\approx \sum_{j=1}^p \begin{pmatrix} c_1 \hat{\gamma}_j^2 / s_j^2 & 0 \\ 0 & c_2 \hat{\gamma}_j^2 / s_j^4 \end{pmatrix}, \text{ and} \\ \nabla \tilde{\mathbf{C}}(\boldsymbol{\theta}) &\approx \sum_{j=1}^p \begin{pmatrix} [\psi_1(t_j) \cdot (\partial/\partial\beta) \hat{\gamma}_j + \hat{\gamma}_j \psi_1'(t_j) \cdot (\partial/\partial\beta) t_j] / s_j & [\psi_1(t_j) \cdot (\partial/\partial\tau^2) \hat{\gamma}_j] / s_j \\ 0 & (\delta + c_3) / (2s_j^4) \end{pmatrix}. \end{aligned} \quad (6)$$

The subscript EB and the dependence of s_j and t_j on $\boldsymbol{\theta}$ are suppressed to simplify the expressions. The constants appeared in (6) are $\delta = \mathbb{E}[\psi_2(Z)]$, $c_1 = \mathbb{E}[\psi_1^2(Z)]$, $c_2 = \text{Var}(\psi_2(Z))$, $c_3 = \mathbb{E}[Z\psi'(Z) - \psi(Z)]$ for $Z \sim \text{N}(0, 1)$. Assuming $\hat{\boldsymbol{\theta}}$ is a good estimator of $\boldsymbol{\theta}$, the matrices in (6) can be estimated by replacing $\boldsymbol{\theta}$ with $\hat{\boldsymbol{\theta}}$.

A.2.5 Diagnostics

To check the modeling assumptions we propose to use a scatterplot of standardized residuals $t_j(\hat{\beta}, \hat{\tau}^2)$ versus the empirical Bayes estimates $\hat{\gamma}_{j,\text{EB}}(\hat{\beta}, \hat{\tau}^2)$, $j = 1, \dots, p$. Note that both t_j and $\hat{\gamma}_{j,\text{EB}}$ depend on the allele coding. To ease the visualization, we choose the allele coding such that $\hat{\gamma}_{j,\text{EB}}$ is positive. Under our modeling assumptions, if $(\hat{\beta}, \hat{\tau}^2)$ is close to the true value, most of $t_j(\hat{\beta}, \hat{\tau}^2)$ should be independent of $\hat{\gamma}_{j,\text{EB}}(\hat{\beta}, \hat{\tau}^2)$ and distributed like a standard normal. We can verify this implication by computing a smoothing spline of the scatter-plot and check it is different from the x -axis (constant 0). More specifically, we run a linear regression with B-splines of $t_j(\hat{\beta}, \hat{\tau}^2)$ with degrees of freedom $\lfloor p/50 \rfloor$ and report the F -test result as “heterogeneity p -value”. We also use the Q-Q plot of $t_j(\hat{\beta}, \hat{\tau}^2)$ against standard normal to check if there is excessive pleiotropy that could not be explained by the normal random effects model.

B Data availability

BMI (Jap): GWAS summary dataset is downloaded from ftp://ftp.ebi.ac.uk/pub/databases/gwas/summary_statistics/AkiyamaM_28892062_GCST004904.

BMI (UKB) and MI (UKB): Round 2 GWAS summary results for the UK BioBank data are available at <http://www.nealelab.is/uk-biobank/>.

LDL-C (2010), HDL-C (2010), and TG (2010): GWAS summary dataset is downloaded from <http://csg.sph.umich.edu/willer/public/lipids2010/>.

LDL-C (2010), HDL-C (2010), and TG (2010): GWAS summary results for the Metabochip data are downloaded from <http://csg.sph.umich.edu/willer/public/lipids2013/>.

CAD: GWAS summary dataset is downloaded from the CARDIoGRAMplusC4D Consortium website: <http://www.cardiogramplusc4d.org/data-downloads/>.

IS: GWAS summary results for the European samples are downloaded from ftp://ftp.ebi.ac.uk/pub/databases/gwas/summary_statistics/MalikR_29531354_GCST005843.

C Detailed results

C.1 Results

In Tables C1 to C5, we report detailed results of our MR analyses.

	$p_{\text{sel}} \in (0, 1)$		$p_{\text{sel}} \in (0, 5 \times 10^{-8})$		$p_{\text{sel}} \in (5 \times 10^{-8}, 1)$	
# SNPs	1119		44		1075	
p_1	0.84		0.81		0.52	
σ_1	1.41		6.55		0.69	
σ_2	5.57		14.22		2.82	
MR-Egger	0.386 (0.077)		0.513 (0.184)		0.442 (0.105)	
Wtd. Med.	0.284 (0.1)		0.278 (0.124)		0.348 (0.105)	
	MLE	Shrinkage	MLE	Shrinkage	MLE	Shrinkage
$\tau_2 = 0, \psi_I$	0.382 (0.061)	0.388 (0.06)	0.291 (0.086)	0.292 (0.086)	0.447 (0.084)	0.454 (0.082)
$\tau_2 = 0, \psi_H$	0.398 (0.061)	0.401 (0.061)	0.345 (0.088)	0.346 (0.088)	0.446 (0.084)	0.452 (0.083)
$\tau_2 \neq 0, \psi_I$	0.367 (0.067)	0.374 (0.066)	0.297 (0.12)	0.298 (0.12)	0.418 (0.09)	0.427 (0.089)
$\tau_2 \neq 0, \psi_H$	0.382 (0.068)	0.387 (0.068)	0.332 (0.117)	0.332 (0.117)	0.42 (0.092)	0.426 (0.091)

(a) Screening: BMI (Dataset: Akiyama et al. (2017)); Exposure: BMI (Dataset: UK BioBank); Outcome: CAD, (Dataset: CARDIoGRAMplusC4D).

	$p_{\text{sel}} \in (0, 1)$		$p_{\text{sel}} \in (0, 5 \times 10^{-8})$		$p_{\text{sel}} \in (5 \times 10^{-8}, 1)$	
# SNPs	1880		63		1817	
p_1	0.88		0.81		0.77	
σ_1	1.2		5.38		0.94	
σ_2	5.35		13.05		3.07	
MR-Egger	0.13 (0.056)		0.193 (0.122)		0.101 (0.076)	
Wtd. Med.	0.112 (0.094)		0.11 (0.107)		0.205 (0.087)	
	MLE	Shrinkage	MLE	Shrinkage	MLE	Shrinkage
$\tau_2 = 0, \psi_I$	0.149 (0.05)	0.157 (0.049)	0.157 (0.071)	0.156 (0.071)	0.144 (0.069)	0.154 (0.068)
$\tau_2 = 0, \psi_H$	0.166 (0.051)	0.177 (0.05)	0.176 (0.073)	0.175 (0.073)	0.158 (0.07)	0.175 (0.069)
$\tau_2 \neq 0, \psi_I$	0.148 (0.051)	0.156 (0.051)	0.157 (0.083)	0.157 (0.083)	0.142 (0.07)	0.152 (0.069)
$\tau_2 \neq 0, \psi_H$	0.163 (0.053)	0.174 (0.052)	0.177 (0.082)	0.176 (0.082)	0.153 (0.072)	0.169 (0.071)

(b) Screening: BMI (Dataset: Akiyama et al. (2017)); Exposure: BMI (Dataset: UK BioBank); Outcome: IS (Dataset: Malik et al. (2018)).

Table C1: Comparison of different MR methods to estimate the effects of Body Mass Index (BMI) on Coronary Artery Disease (CAD) and ischemic stroke (IS).

	$p_{\text{sel}} \in (0, 1)$		$p_{\text{sel}} \in (0, 5 \times 10^{-8})$		$p_{\text{sel}} \in (5 \times 10^{-8}, 1)$	
# SNPs	1214		37		1177	
p_1	0.92		0.99		0.85	
σ_1	0.54		10.87		0.34	
σ_2	7.32		10.87		2.08	
MR-Egger	0.3909 (0.0316)		0.5047 (0.0877)		0.0565 (0.0644)	
Wtd. Med.	0.4215 (0.0486)		0.4872 (0.0476)		0.1825 (0.0699)	
	MLE	Shrinkage	MLE	Shrinkage	MLE	Shrinkage
$\tau_2 = 0, \psi_I$	0.475 (0.031)	0.479 (0.029)	0.473 (0.029)	0.473 (0.029)	0.489 (0.164)	0.535 (0.134)
$\tau_2 = 0, \psi_H$	0.499 (0.031)	0.497 (0.028)	0.49 (0.029)	0.49 (0.029)	0.562 (0.126)	0.567 (0.106)
$\tau_2 \neq 0, \psi_I$	0.424 (0.033)	0.449 (0.032)	0.445 (0.047)	0.445 (0.047)	0.259 (0.109)	0.329 (0.116)
$\tau_2 \neq 0, \psi_H$	0.458 (0.033)	0.477 (0.031)	0.476 (0.043)	0.476 (0.043)	0.345 (0.11)	0.42 (0.102)

(a) Screening: LDL-C (Dataset: Teslovich et al. (2010)); Exposure: LDL-C (Dataset: Metabochip, Willer et al. (2013)); Outcome: CAD, (Dataset: CARDIoGRAMplusC4D).

	$p_{\text{sel}} \in (0, 1)$		$p_{\text{sel}} \in (0, 5 \times 10^{-8})$		$p_{\text{sel}} \in (5 \times 10^{-8}, 1)$	
# SNPs	1191		42		1149	
p_1	0.89		0.01		0.86	
σ_1	0.72		8.94		0.61	
σ_2	5.75		8.94		2.82	
MR-Egger	-0.172 (0.0364)		0.1911 (0.1138)		-0.2896 (0.0597)	
Wtd. Med.	0.0111 (0.056)		0.0461 (0.0691)		-0.0824 (0.0615)	
	MLE	Shrinkage	MLE	Shrinkage	MLE	Shrinkage
$\tau_2 = 0, \psi_I$	-0.25 (0.034)	-0.212 (0.032)	-0.151 (0.035)	-0.151 (0.035)	-0.479 (0.078)	-0.421 (0.07)
$\tau_2 = 0, \psi_H$	-0.325 (0.033)	-0.275 (0.031)	-0.238 (0.035)	-0.238 (0.035)	-0.431 (0.071)	-0.349 (0.065)
$\tau_2 \neq 0, \psi_I$	-0.229 (0.037)	-0.201 (0.036)	-0.171 (0.069)	-0.171 (0.069)	-0.383 (0.073)	-0.35 (0.069)
$\tau_2 \neq 0, \psi_H$	-0.282 (0.036)	-0.245 (0.035)	-0.201 (0.07)	-0.201 (0.07)	-0.353 (0.072)	-0.294 (0.067)

(b) Screening: HDL-C (Dataset: Teslovich et al. (2010)); Exposure: HDL-C (Dataset: Metabochip, Willer et al. (2013)); Outcome: CAD, (Dataset: CARDIoGRAMplusC4D).

	$p_{\text{sel}} \in (0, 1)$		$p_{\text{sel}} \in (0, 5 \times 10^{-8})$		$p_{\text{sel}} \in (5 \times 10^{-8}, 1)$	
# SNPs	1194		28		1166	
p_1	0.95		0.01		0.83	
σ_1	0.61		11.48		0.27	
σ_2	8.21		11.48		1.93	
MR-Egger	0.2037 (0.0355)		0.0881 (0.0865)		0.2767 (0.0761)	
Wtd. Med.	0.1784 (0.054)		0.1761 (0.0511)		0.219 (0.0815)	
	MLE	Shrinkage	MLE	Shrinkage	MLE	Shrinkage
$\tau_2 = 0, \psi_I$	0.313 (0.036)	0.261 (0.032)	0.202 (0.032)	0.202 (0.032)	1.179 (0.19)	1.039 (0.181)
$\tau_2 = 0, \psi_H$	0.344 (0.035)	0.268 (0.032)	0.213 (0.033)	0.213 (0.033)	1.091 (0.156)	0.987 (0.134)
$\tau_2 \neq 0, \psi_I$	0.277 (0.038)	0.248 (0.036)	0.217 (0.051)	0.217 (0.051)	0.7 (0.144)	0.709 (0.127)
$\tau_2 \neq 0, \psi_H$	0.288 (0.038)	0.255 (0.036)	0.217 (0.055)	0.217 (0.055)	0.726 (0.145)	0.735 (0.125)

(c) Screening: TG (Dataset: Teslovich et al. (2010)); Exposure: TG (Dataset: Metabochip, Willer et al. (2013)); Outcome: CAD, (Dataset: CARDIoGRAMplusC4D).

Table C2: Comparison of different MR methods to estimate the effects of blood lipid levels on Coronary Artery Disease (CAD) using the CARDIoGRAMplusC4D dataset and unrestricted instruments.

	$p_{\text{sel}} \in (0, 1)$		$p_{\text{sel}} \in (0, 5 \times 10^{-8})$		$p_{\text{sel}} \in (5 \times 10^{-8}, 1)$	
# SNPs	898		11		887	
p_1	0.92		0.01		0.92	
σ_1	0.47		5.93		0.44	
σ_2	3.38		5.93		2.39	
MR-Egger	0.3167 (0.0614)		0.7336 (0.3916)		0.2563 (0.0731)	
Wtd. Med.	0.3027 (0.0821)		0.4638 (0.1241)		0.2291 (0.0786)	
	MLE	Shrinkage	MLE	Shrinkage	MLE	Shrinkage
$\tau_2 = 0, \psi_I$	0.432 (0.089)	0.504 (0.081)	0.419 (0.101)	0.419 (0.101)	0.443 (0.135)	0.577 (0.13)
$\tau_2 = 0, \psi_H$	0.364 (0.085)	0.483 (0.076)	0.44 (0.098)	0.44 (0.098)	0.29 (0.126)	0.514 (0.116)
$\tau_2 \neq 0, \psi_I$	0.393 (0.086)	0.482 (0.08)	0.449 (0.167)	0.449 (0.167)	0.395 (0.128)	0.538 (0.123)
$\tau_2 \neq 0, \psi_H$	0.348 (0.085)	0.471 (0.077)	0.452 (0.167)	0.452 (0.167)	0.277 (0.126)	0.498 (0.116)

(a) Screening: LDL-C (Dataset: Teslovich et al. (2010)); Exposure: LDL-C (Dataset: Metabochip, Willer et al. (2013)); Outcome: CAD, (Dataset: CARDIoGRAMplusC4D).

	$p_{\text{sel}} \in (0, 1)$		$p_{\text{sel}} \in (0, 5 \times 10^{-8})$		$p_{\text{sel}} \in (5 \times 10^{-8}, 1)$	
# SNPs	869		8		861	
p_1	0.95		0.01		0.93	
σ_1	0.68		7.07		0.65	
σ_2	3.88		7.07		2.38	
MR-Egger	-0.0757 (0.0704)		-0.1905 (0.3977)		-0.057 (0.0839)	
Wtd. Med.	-0.1496 (0.0812)		-0.0792 (0.1235)		-0.1836 (0.0861)	
	MLE	Shrinkage	MLE	Shrinkage	MLE	Shrinkage
$\tau_2 = 0, \psi_I$	-0.402 (0.107)	-0.377 (0.086)	-0.142 (0.097)	-0.142 (0.097)	-0.622 (0.182)	-0.676 (0.155)
$\tau_2 = 0, \psi_H$	-0.419 (0.094)	-0.38 (0.081)	-0.139 (0.1)	-0.139 (0.1)	-0.651 (0.143)	-0.707 (0.13)
$\tau_2 \neq 0, \psi_I$	-0.276 (0.093)	-0.296 (0.085)	-0.142 (0.097)	-0.142 (0.097)	-0.348 (0.13)	-0.43 (0.124)
$\tau_2 \neq 0, \psi_H$	-0.318 (0.092)	-0.318 (0.085)	-0.139 (0.1)	-0.139 (0.1)	-0.447 (0.131)	-0.53 (0.125)

(b) Screening: HDL-C (Dataset: Teslovich et al. (2010)); Exposure: HDL-C (Dataset: Metabochip, Willer et al. (2013)); Outcome: CAD, (Dataset: CARDIoGRAMplusC4D).

	$p_{\text{sel}} \in (0, 1)$		$p_{\text{sel}} \in (0, 5 \times 10^{-8})$		$p_{\text{sel}} \in (5 \times 10^{-8}, 1)$	
# SNPs	881		2		879	
p_1	0.99		0.01		0.98	
σ_1	0.4		8.3		0.38	
σ_2	4.58		8.3		2.49	
MR-Egger	0.0787 (0.0822)		-0.1803 (0.1427)		0.1616 (0.0935)	
Wtd. Med.	-0.0195 (0.1264)		-0.1803 (0.1427)		0.1299 (0.0948)	
	MLE	Shrinkage	MLE	Shrinkage	MLE	Shrinkage
$\tau_2 = 0, \psi_I$	0.207 (0.259)	0.046 (0.136)	-0.182 (0.144)	-0.182 (0.144)	0.886 (0.657)	0.852 (0.374)
$\tau_2 = 0, \psi_H$	0.25 (0.225)	-0.064 (0.132)	-0.182 (0.148)	-0.182 (0.148)	0.77 (0.46)	0.972 (0.333)
$\tau_2 \neq 0, \psi_I$	0.142 (0.187)	0.044 (0.136)	-0.182 (0.144)	-0.182 (0.144)	0.381 (0.307)	0.555 (0.255)
$\tau_2 \neq 0, \psi_H$	0.159 (0.192)	-0.047 (0.136)	-0.182 (0.148)	-0.182 (0.148)	0.385 (0.315)	0.464 (0.256)

(c) Screening: TG (Dataset: Teslovich et al. (2010)); Exposure: TG (Dataset: Metabochip, Willer et al. (2013)); Outcome: CAD, (Dataset: CARDIoGRAMplusC4D).

Table C3: Comparison of different MR methods to estimate the effects of blood lipid levels on Coronary Artery Disease (CAD) using the CARDIoGRAMplusC4D dataset and restricted instruments.

	$p_{\text{sel}} \in (0, 1)$		$p_{\text{sel}} \in (0, 5 \times 10^{-8})$		$p_{\text{sel}} \in (5 \times 10^{-8}, 1)$	
# SNPs	1140		37		1103	
p_1	0.92		0.99		0.87	
σ_1	0.55		10.87		0.4	
σ_2	7.27		10.87		2.34	
MR-Egger	0.011 (0.0011)		0.0127 (0.0023)		0.0047 (0.0024)	
Wtd. Med.	0.0122 (0.0017)		0.0124 (0.0016)		0.0061 (0.0027)	
	MLE	Shrinkage	MLE	Shrinkage	MLE	Shrinkage
$\tau_2 = 0, \psi_I$	0.012 (0.001)	0.012 (0.001)	0.012 (0.001)	0.012 (0.001)	0.014 (0.005)	0.013 (0.004)
$\tau_2 = 0, \psi_H$	0.013 (0.001)	0.013 (0.001)	0.013 (0.001)	0.013 (0.001)	0.015 (0.004)	0.014 (0.003)
$\tau_2 \neq 0, \psi_I$	0.012 (0.001)	0.012 (0.001)	0.012 (0.001)	0.012 (0.001)	0.01 (0.004)	0.01 (0.003)
$\tau_2 \neq 0, \psi_H$	0.012 (0.001)	0.012 (0.001)	0.013 (0.001)	0.013 (0.001)	0.01 (0.004)	0.011 (0.003)

(a) Screening: LDL-C (Dataset: Teslovich et al. (2010)); Exposure: LDL-C (Dataset: Metabochip, Willer et al. (2013)); Outcome: CAD, (Dataset: UK BioBank).

	$p_{\text{sel}} \in (0, 1)$		$p_{\text{sel}} \in (0, 5 \times 10^{-8})$		$p_{\text{sel}} \in (5 \times 10^{-8}, 1)$	
# SNPs	1079		39		1040	
p_1	0.89		0.01		0.85	
σ_1	0.76		9.15		0.64	
σ_2	5.9		9.15		2.81	
MR-Egger	-0.0056 (0.0013)		0.0094 (0.0043)		-0.0112 (0.0022)	
Wtd. Med.	-0.0018 (0.0019)		-7e-04 (0.0025)		-0.0044 (0.0024)	
	MLE	Shrinkage	MLE	Shrinkage	MLE	Shrinkage
$\tau_2 = 0, \psi_I$	-0.007 (0.001)	-0.007 (0.001)	-0.004 (0.001)	-0.004 (0.001)	-0.014 (0.003)	-0.014 (0.002)
$\tau_2 = 0, \psi_H$	-0.009 (0.001)	-0.008 (0.001)	-0.006 (0.001)	-0.006 (0.001)	-0.012 (0.003)	-0.011 (0.002)
$\tau_2 \neq 0, \psi_I$	-0.007 (0.001)	-0.006 (0.001)	-0.004 (0.003)	-0.004 (0.003)	-0.013 (0.003)	-0.014 (0.002)
$\tau_2 \neq 0, \psi_H$	-0.009 (0.001)	-0.008 (0.001)	-0.004 (0.003)	-0.004 (0.003)	-0.011 (0.003)	-0.011 (0.002)

(b) Screening: HDL-C (Dataset: Teslovich et al. (2010)); Exposure: HDL-C (Dataset: Metabochip, Willer et al. (2013)); Outcome: CAD, (Dataset: UK BioBank).

	$p_{\text{sel}} \in (0, 1)$		$p_{\text{sel}} \in (0, 5 \times 10^{-8})$		$p_{\text{sel}} \in (5 \times 10^{-8}, 1)$	
# SNPs	1122		27		1095	
p_1	0.95		0.01		0.84	
σ_1	0.64		11.68		0.34	
σ_2	8.26		11.68		1.99	
MR-Egger	0.0088 (0.0013)		0.0032 (0.0035)		0.0139 (0.0027)	
Wtd. Med.	0.0072 (0.0019)		0.0072 (0.0018)		0.0087 (0.003)	
	MLE	Shrinkage	MLE	Shrinkage	MLE	Shrinkage
$\tau_2 = 0, \psi_I$	0.013 (0.001)	0.011 (0.001)	0.008 (0.001)	0.008 (0.001)	0.033 (0.005)	0.03 (0.004)
$\tau_2 = 0, \psi_H$	0.013 (0.001)	0.011 (0.001)	0.008 (0.001)	0.008 (0.001)	0.03 (0.004)	0.026 (0.004)
$\tau_2 \neq 0, \psi_I$	0.012 (0.001)	0.01 (0.001)	0.007 (0.002)	0.007 (0.002)	0.029 (0.005)	0.027 (0.004)
$\tau_2 \neq 0, \psi_H$	0.012 (0.001)	0.01 (0.001)	0.007 (0.002)	0.007 (0.002)	0.027 (0.005)	0.024 (0.004)

(c) Screening: TG (Dataset: Teslovich et al. (2010)); Exposure: TG (Dataset: Metabochip, Willer et al. (2013)); Outcome: CAD, (Dataset: UK BioBank).

Table C4: Comparison of different MR methods to estimate the effects of blood lipid levels on Coronary Artery Disease (CAD) using the UK BioBank dataset and unrestricted instruments.

	$p_{\text{sel}} \in (0, 1)$		$p_{\text{sel}} \in (0, 5 \times 10^{-8})$		$p_{\text{sel}} \in (5 \times 10^{-8}, 1)$	
# SNPs	835		11		824	
p_1	0.92		0.01		0.92	
σ_1	0.45		5.93		0.42	
σ_2	3.41		5.93		2.41	
MR-Egger	0.0108 (0.0025)		0.0165 (0.0132)		0.0095 (0.0029)	
Wtd. Med.	0.006 (0.0033)		0.0068 (0.0049)		0.0067 (0.0033)	
	MLE	Shrinkage	MLE	Shrinkage	MLE	Shrinkage
$\tau_2 = 0, \psi_I$	0.015 (0.004)	0.014 (0.003)	0.013 (0.004)	0.013 (0.004)	0.018 (0.006)	0.016 (0.006)
$\tau_2 = 0, \psi_H$	0.015 (0.004)	0.013 (0.003)	0.012 (0.004)	0.012 (0.004)	0.018 (0.006)	0.017 (0.005)
$\tau_2 \neq 0, \psi_I$	0.014 (0.004)	0.014 (0.003)	0.014 (0.006)	0.014 (0.006)	0.015 (0.006)	0.015 (0.005)
$\tau_2 \neq 0, \psi_H$	0.013 (0.004)	0.013 (0.003)	0.014 (0.006)	0.014 (0.006)	0.015 (0.005)	0.015 (0.005)

(a) Screening: LDL-C (Dataset: Teslovich et al. (2010)); Exposure: LDL-C (Dataset: Metabochip, Willer et al. (2013)); Outcome: CAD, (Dataset: UK BioBank).

	$p_{\text{sel}} \in (0, 1)$		$p_{\text{sel}} \in (0, 5 \times 10^{-8})$		$p_{\text{sel}} \in (5 \times 10^{-8}, 1)$	
# SNPs	800		7		793	
p_1	0.95		0.01		0.95	
σ_1	0.68		7.09		0.66	
σ_2	3.99		7.09		2.59	
MR-Egger	-0.0054 (0.0025)		0.0088 (0.0157)		-0.0077 (0.003)	
Wtd. Med.	-0.0065 (0.0032)		-0.0055 (0.005)		-0.0084 (0.0034)	
	MLE	Shrinkage	MLE	Shrinkage	MLE	Shrinkage
$\tau_2 = 0, \psi_I$	-0.012 (0.003)	-0.011 (0.003)	-0.001 (0.004)	-0.001 (0.004)	-0.018 (0.005)	-0.021 (0.004)
$\tau_2 = 0, \psi_H$	-0.015 (0.003)	-0.013 (0.003)	-0.003 (0.004)	-0.003 (0.004)	-0.022 (0.005)	-0.024 (0.004)
$\tau_2 \neq 0, \psi_I$	-0.011 (0.003)	-0.011 (0.003)	-0.001 (0.004)	-0.001 (0.004)	-0.017 (0.005)	-0.02 (0.004)
$\tau_2 \neq 0, \psi_H$	-0.014 (0.003)	-0.013 (0.003)	-0.003 (0.004)	-0.003 (0.004)	-0.02 (0.005)	-0.023 (0.005)

(b) Screening: HDL-C (Dataset: Teslovich et al. (2010)); Exposure: HDL-C (Dataset: Metabochip, Willer et al. (2013)); Outcome: CAD, (Dataset: UK BioBank).

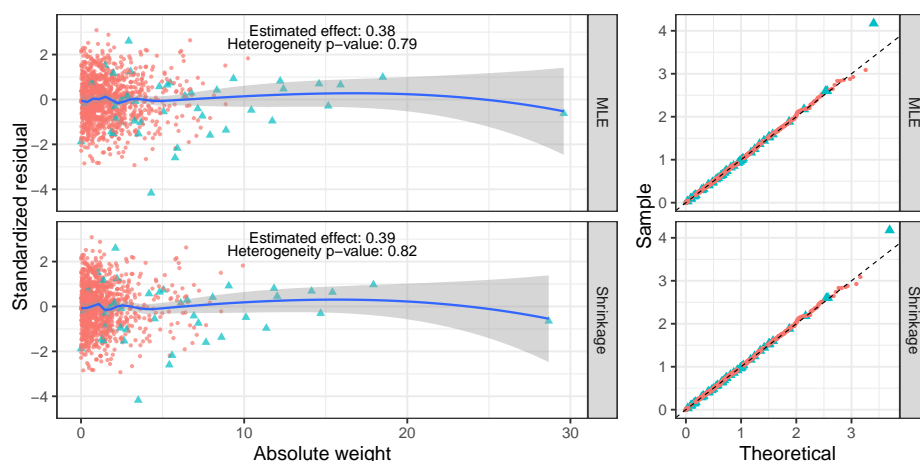
	$p_{\text{sel}} \in (0, 1)$		$p_{\text{sel}} \in (0, 5 \times 10^{-8})$		$p_{\text{sel}} \in (5 \times 10^{-8}, 1)$	
# SNPs	801		2		799	
p_1	0.99		0.01		0.95	
σ_1	0.4		8.3		0.32	
σ_2	4.4		8.3		1.61	
MR-Egger	0.0059 (0.0033)		0.0036 (0.0056)		0.0068 (0.0038)	
Wtd. Med.	0.0064 (0.0042)		0.0036 (0.0056)		0.0043 (0.0039)	
	MLE	Shrinkage	MLE	Shrinkage	MLE	Shrinkage
$\tau_2 = 0, \psi_I$	0.026 (0.009)	0.007 (0.005)	0.004 (0.006)	0.004 (0.006)	0.046 (0.016)	0.025 (0.017)
$\tau_2 = 0, \psi_H$	0.032 (0.009)	0.005 (0.005)	0.004 (0.006)	0.004 (0.006)	0.049 (0.017)	0.03 (0.015)
$\tau_2 \neq 0, \psi_I$	0.021 (0.007)	0.006 (0.005)	0.004 (0.006)	0.004 (0.006)	0.033 (0.013)	0.018 (0.011)
$\tau_2 \neq 0, \psi_H$	0.019 (0.008)	0.005 (0.005)	0.004 (0.006)	0.004 (0.006)	0.03 (0.014)	0.017 (0.012)

(c) Screening: TG (Dataset: Teslovich et al. (2010)); Exposure: TG (Dataset: Metabochip, Willer et al. (2013)); Outcome: CAD, (Dataset: UK BioBank).

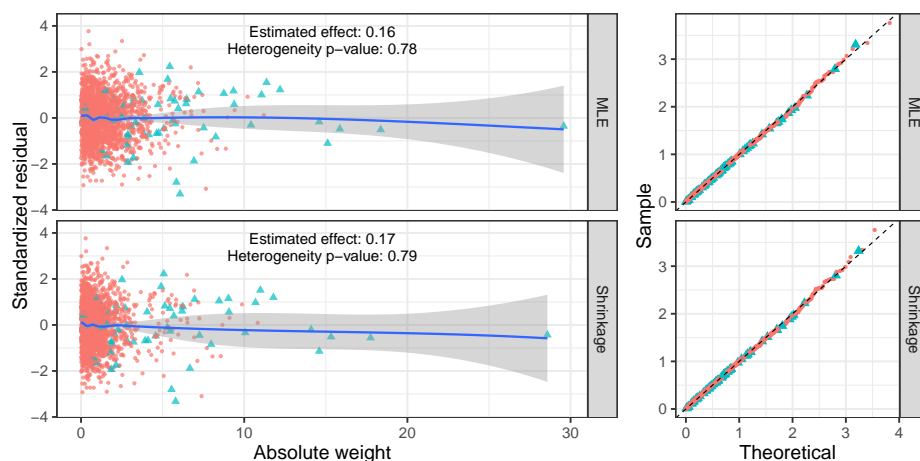
Table C5: Comparison of different MR methods to estimate the effects of blood lipid levels on Coronary Artery Disease (CAD) using the UK BioBank dataset and restricted instruments.

C.2 Diagnostic plots

Figures C1 to C5 below are diagnostic plots to check instrument heterogeneity. If our modeling assumptions are satisfied, most of the standardized residuals (y -axis) should be approximately independent of the instrument weight (x -axis), checked by the scatter-plot in the left panel of each figure, and should roughly follow the standard normal distribution, checked by the quantile-quantile plot in the right panel of each figure. The heterogeneity p -values are computed by testing the null model in the linear regression of the standardized residual on the absolute weight (expanded using B-splines with degrees of freedom equal to $\#instruments/20$).

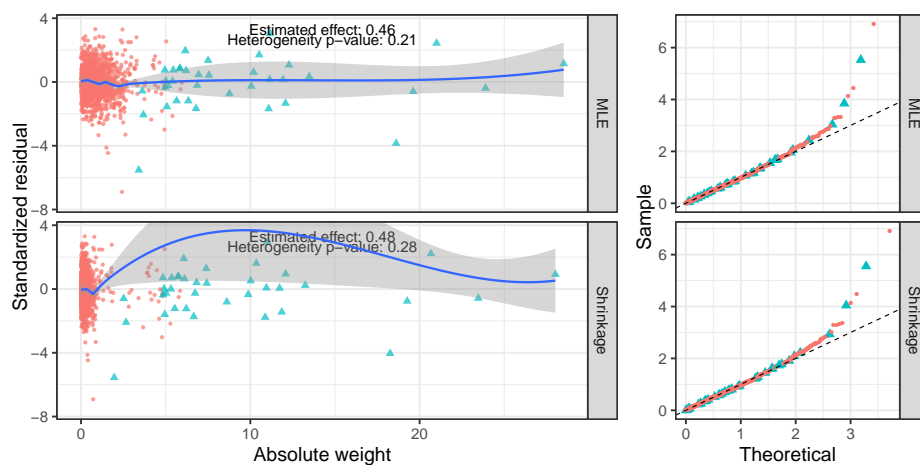


(a) Screening: BMI (Dataset: Akiyama et al. (2017)); Exposure: BMI (Dataset: UK BioBank); Outcome: CAD, (Dataset: CARDIoGRAMplusC4D).

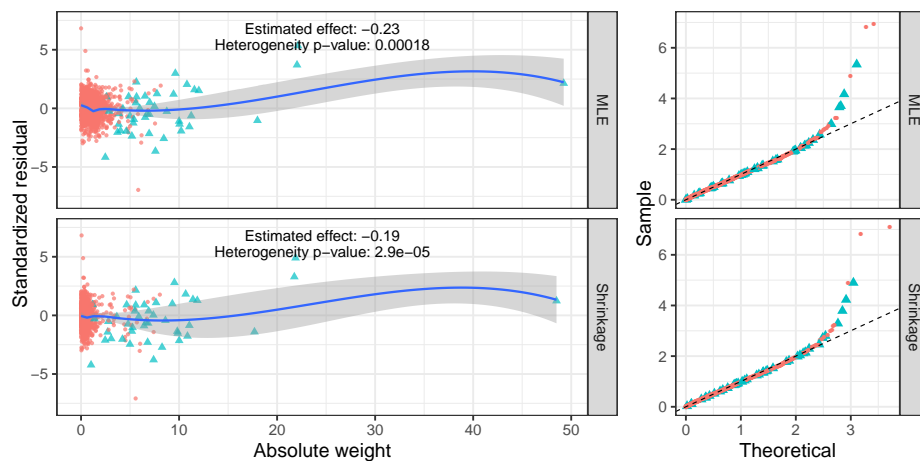


(b) Screening: BMI (Dataset: Akiyama et al. (2017)); Exposure: BMI (Dataset: UK BioBank); Outcome: IS (Dataset: Malik et al. (2018)).

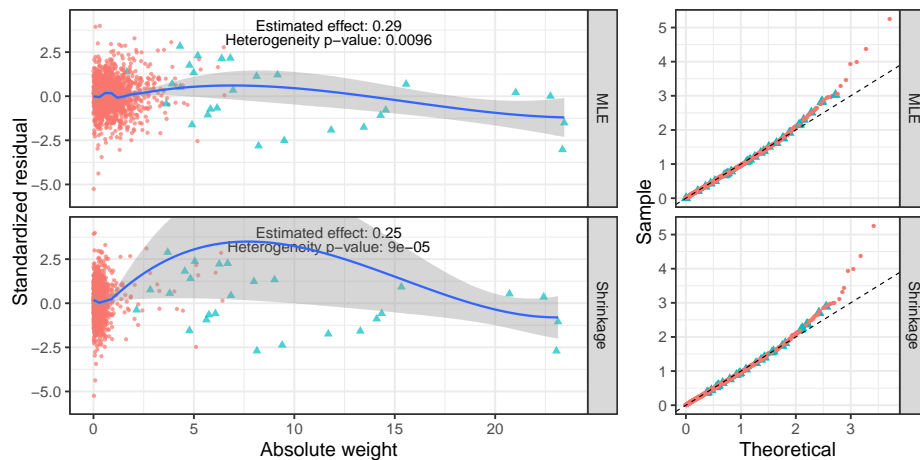
Figure C1: Diagnostic plots for the BMI results.



(a) LDL-c.

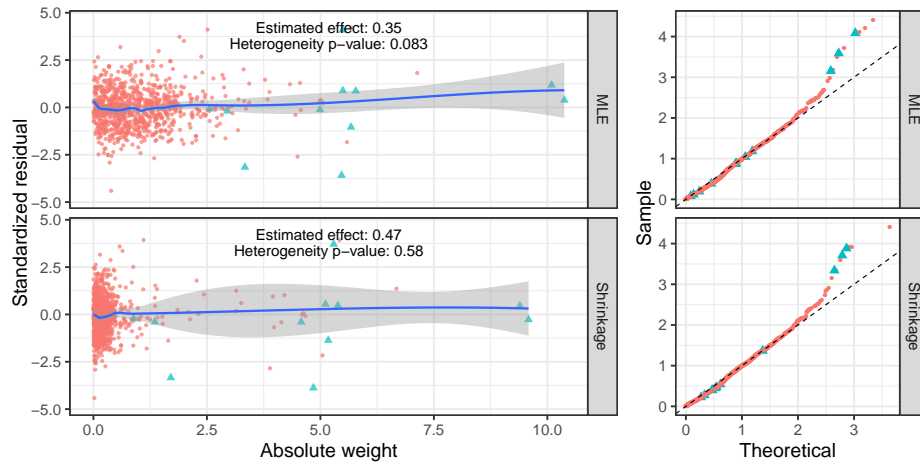


(b) HDL-c.

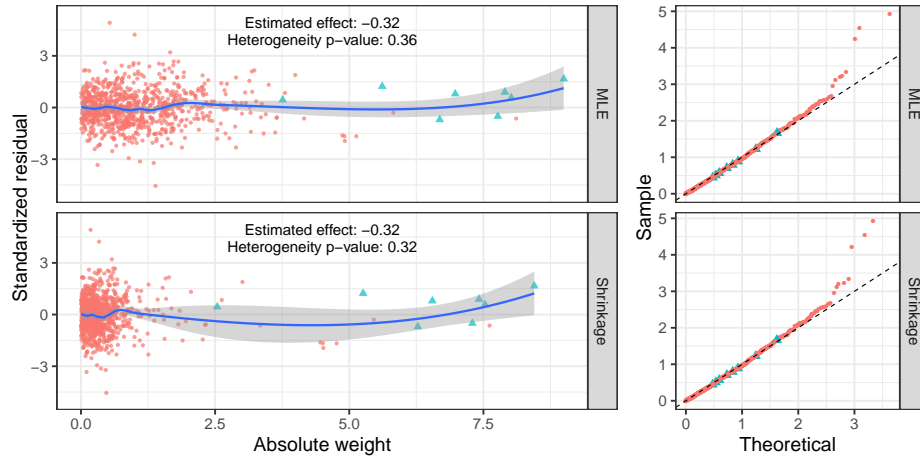


(c) TG.

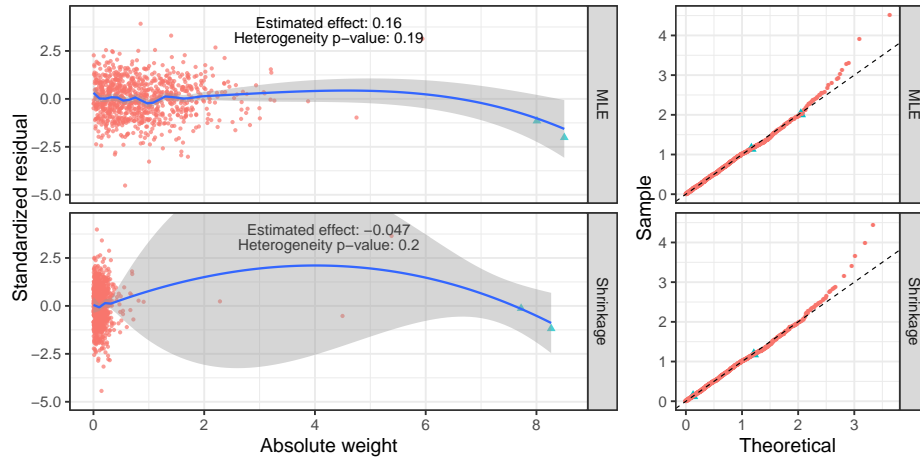
Figure C2: Diagnostic plots for the lipids results using unrestricted instruments and the CARDIoGRAMplusC4D dataset.



(a) LDL-c.

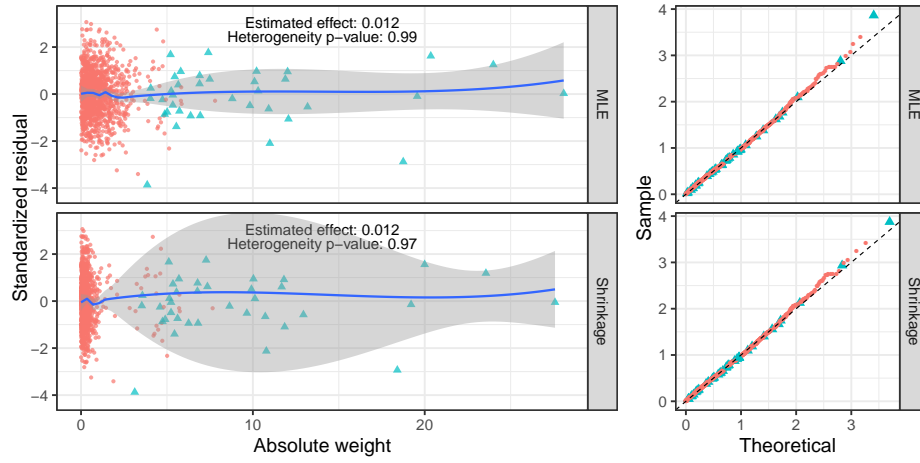


(b) HDL-c.

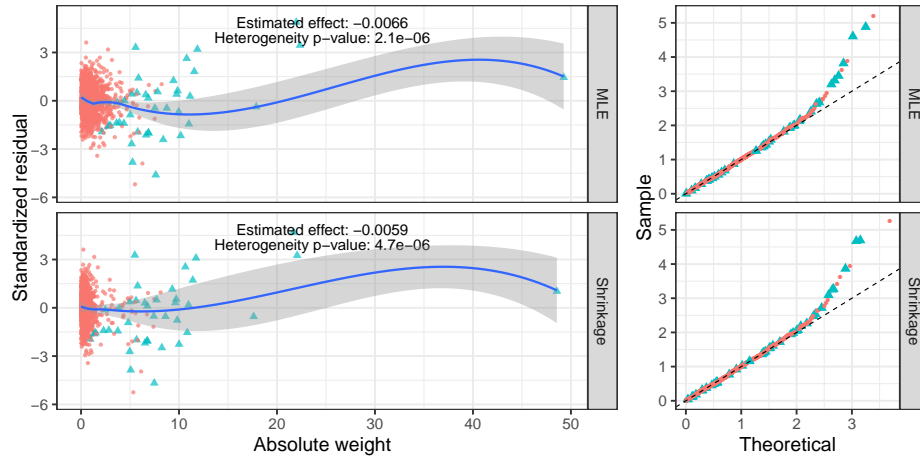


(c) TG.

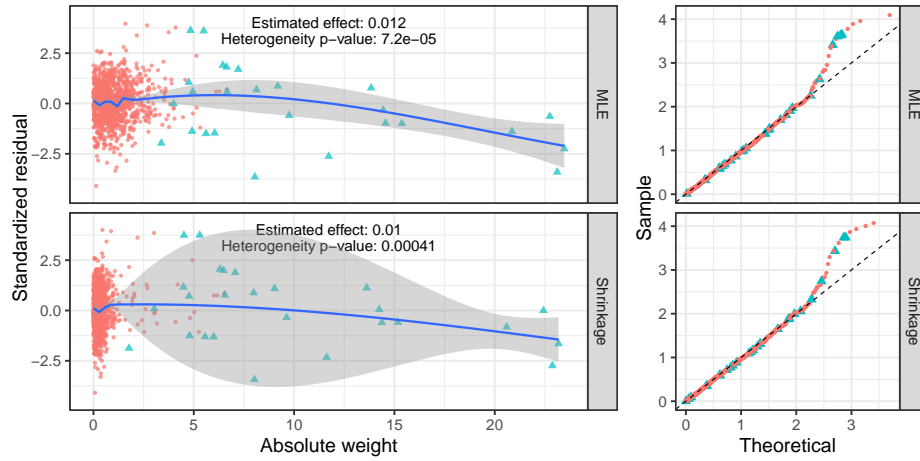
Figure C3: Diagnostic plots for the lipids results using restricted instruments and the CARDIoGRAMplusC4D dataset.



(a) LDL-c.

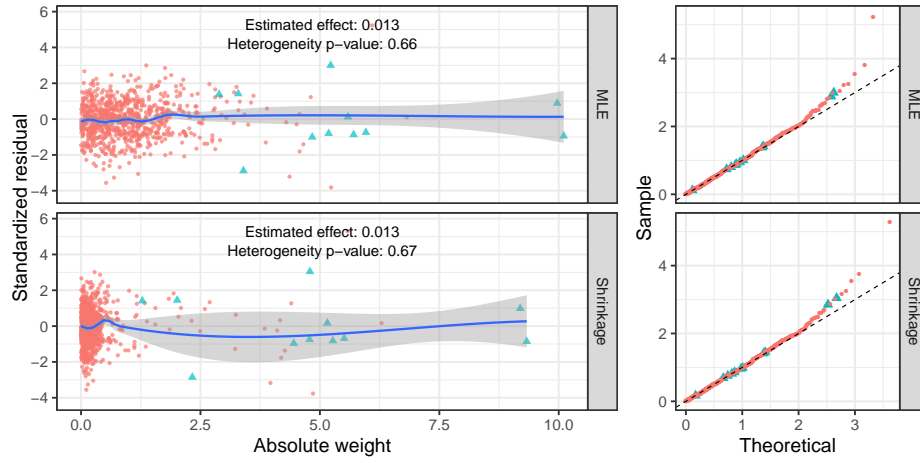


(b) HDL-c.

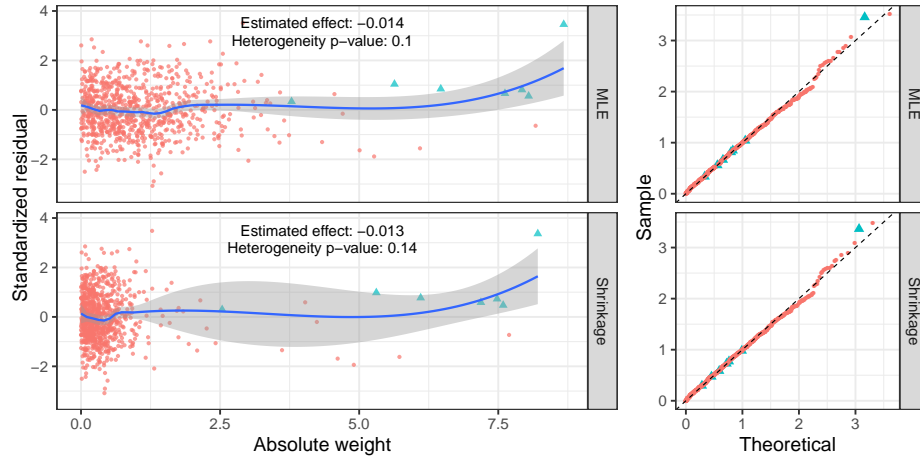


(c) TG.

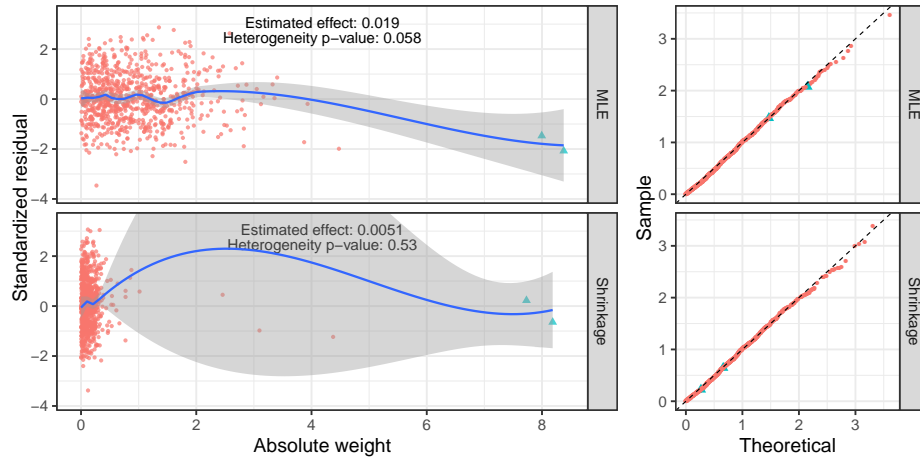
Figure C4: Diagnostic plots for the lipids results using unrestricted instruments and the UK BioBank dataset dataset.



(a) LDL-c.



(b) HDL-c.



(c) TG.

Figure C5: Diagnostic plots for the lipids results using restricted instruments and the UK BioBank dataset.